

Quantifying effectiveness of trees for landslide erosion control

Raphael I. Spiekermann^{a,b,*}, Hugh G. Smith^a, Sam McColl^b, Lucy Burkitt^b, Ian C. Fuller^b

^a Manaaki Whenua – Landcare Research, Palmerston North, New Zealand

^b School of Agriculture and Environment, Massey University, Palmerston North, New Zealand

ARTICLE INFO

Article history:

Received 20 June 2021

Received in revised form 26 September 2021

Accepted 11 October 2021

Available online 15 October 2021

Keywords:

Landslide susceptibility
erosion mitigation
Silvopastoralism
Shallow landslides
Individual trees
Binary logistic regression

ABSTRACT

We developed a landslide susceptibility model using binary logistic regression for silvopastoral landscapes, which for the first time includes spatial distribution models for individual trees of different vegetation types. Models were trained and tested using a landslide inventory consisting of 43,000 landslide scars mapped across an 843 km² area. Model performance was very good, with a median AUROC of 0.95 in the final model used for predictions, which equates to an accuracy of 88.7% using a cut-off of 0.5. We investigate the effect of highly skewed continuous tree variables on the maximum likelihood estimator by testing different sampling strategies aimed at reducing positive skewness. With an adequate sample size, we found that highly skewed continuous predictor variables do not result in an inflation of effect size.

Using two farms in the study area, we illustrate application of the landslide susceptibility model for quantifying the reduction in shallow landslide erosion due to trees. Landslide erosion was reduced by 16.6% at Site 1 and 42.9% at Site 2 due to all existing vegetation. The effectiveness of individual trees on reducing landslide erosion was shown to be less a function of species than that of targeting highly susceptible areas with adequate plant densities. We found 80% of landslides are triggered in 12.1% and 7.3% of the area of Sites 1 (1700-ha) and 2 (462-ha), respectively, suggesting there is great potential for smarter targeting of erosion mitigation. The high-resolution spatial information provided by the landslide susceptibility maps can be used by decision makers in land management to support the development and targeting of erosion mitigation measures.

© 2021 Elsevier B.V. All rights reserved.

1. Introduction

Accurately quantifying the effectiveness of trees for hillslope stability remains a key challenge for erosion control research. Irrespective of tree species, methods to quantify the effect of trees on landslide erosion generally use 1) empirical- (e.g., Douglas et al., 2013), 2) physical- (e.g., Schwarz et al., 2016), or 3) statistical-based approaches (e.g., Reichenbach et al., 2014). Quantitative empirical studies have demonstrated and/or modelled that widely spaced trees on hillslopes reduce landslide erosion by 70–95% within 10 m of tree stems compared with untreated control sites (Hawley and Dymond, 1988; Hicks, 1989a, 1989b, 1992; Thompson and Luckman, 1993; Phillips et al., 2008; Douglas et al., 2009, 2013; McIvor et al., 2011, 2015). Yet, such univariate methods do not account for variation in environmental factors and tree densities. Physical models can include root reinforcement modelling to quantify increases in soil shear strength for a given slope (e.g., Schwarz et al., 2012, 2016). Such approaches are well suited to

assessing effectiveness of trees at the hillslope scale but are less practical at regional scales due to the data requirements relating to the physical parameters of the soil which can be highly variable in hilly or steep landscapes (Holcombe et al., 2012; Masi et al., 2021). For larger areas, simplified assumptions must be made (Salvatici et al., 2018), which can result in poorer performance of physical models compared with statistical methods (e.g., Cervi et al., 2010). Therefore, both deterministic and probabilistic approaches that integrate root reinforcement models in slope stability calculations have largely had homogenous protection forests as the object of their investigation (e.g., Cislighi et al., 2017). Probabilistic approaches deal with the variability inherent in input parameters by considering the probability distributions. For example, SlideforMap generates hypothetical landslides of varying sizes to compute slope stability using semi-random samples over pre-defined ranges for soil cohesion, internal friction angle and soil depth (van Zadelhoff et al., 2021). A further novelty of SlideforMap is the inclusion of root reinforcement based on individual tree detection with application at landscape to regional scales. While integrating the influence of individual trees in slope stability calculations has been held in the domain of physical modelling, this study aims to develop a statistical approach for assessing effectiveness of individual trees in silvopastoral landscapes.

* Corresponding author at: Manaaki Whenua – Landcare Research, Palmerston North, New Zealand.

E-mail address: spiekermann@landcareresearch.co.nz (R.I. Spiekermann).

Landslide susceptibility can be defined as the likelihood of future landslide occurrence for a given areal unit given local geo-environmental attributes (Brabb, 1984). Statistical landslide susceptibility models do not attempt to model the physical processes that control slope stability. Rather, and in the absence of geotechnical soil data, statistical models use readily available surrogate data and thus have less stringent data requirements compared with physical models. A key input parameter that influences the accuracy of statistical susceptibility models, especially for evaluating the influence of single trees, is the quality of vegetation data. In most existing statistical models, land use or land cover data (LULC) are used to capture the varying effect of vegetation composition. These data are frequently prepared through visual interpretation of aerial photography and are rarely available at the scale required to quantify the effect of individual trees (Reichenbach et al., 2018; Spiekermann et al., 2021). Therefore, in hill country, where shallow landslide erosion is a dominant geomorphic process (Smith et al., 2021), we address the methodological and knowledge gap related to statistical modelling at landscape scale to quantify the reduction in landslide erosion due to individual trees at landscape scales.

In this context of silvopastoral landscapes, previous studies have been limited by scale (e.g., hillslope) or method (e.g., univariate analyses). There is a need for spatially explicit modelling to assess the impact of differing tree species and planting densities on landslide erosion while accounting for varying environmental conditions, such as slope

gradient, lithology, or soil type. To enable such assessments, high resolution vegetation data are a prerequisite. Automated processing of satellite imagery and airborne LiDAR data is continually increasing the spatial and temporal resolution of land cover products, creating opportunities to map the location of individual trees in the landscape (Gómez et al., 2016; Brandt et al., 2020; Weinstein et al., 2021). However, beyond mapping trees, the challenge for landslide susceptibility models is the spatial representation of trees as predictor variables in the model: Representing individual trees as points/pixels, mapping tree canopies, or using an arbitrary radius to define an area of influence of a tree fail to acknowledge the spatial variation in the distribution and strength of roots as well as the hydrological interactions between trees and soil. While root distribution models have been used for physical, process-based modelling, the cost of data collection is prohibitive and not suited to landscapes with a diverse range of tree species. A solution to this problem was recently proposed by Spiekermann et al. (2021), whereby the average extent and spatial pattern of individual trees on slope stability is inferred by considering the relationship between the location of trees and landslides. The recent availability of the tree influence models (TIMSS) provides an opportunity to create greatly improved landslide susceptibility models for silvopastoral landscapes. Thereby, the increase in slope stability due to individual trees can be quantified, and, inversely, the reduction in landslide susceptibility and erosion. Accounting for the influence of individual trees has been

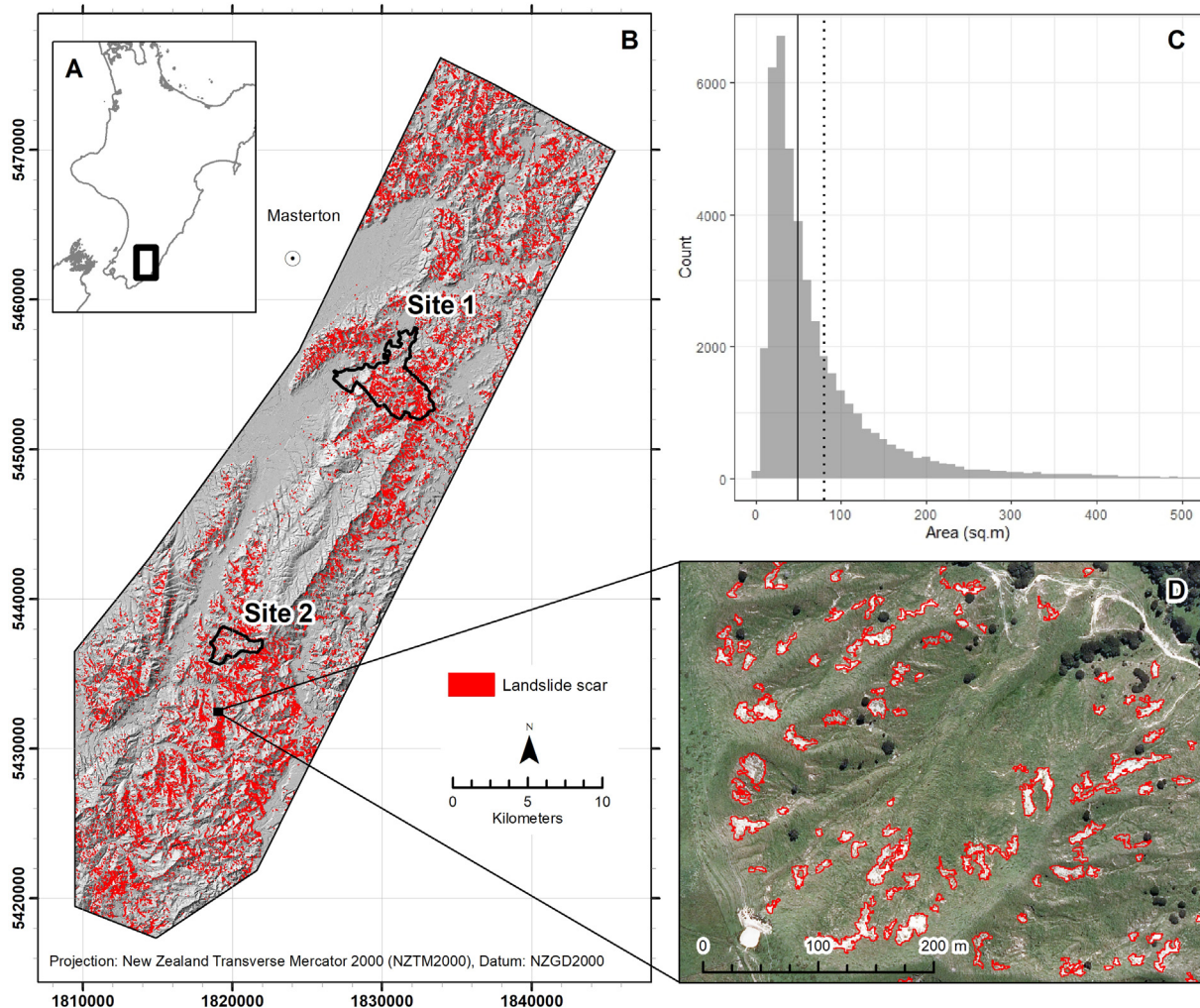


Fig. 1. A: Location of study area in the lower North Island, New Zealand; B: Shallow landslide inventory 2005–2009 used to train landslide susceptibility models; C: Histogram of landslide scar size (bin width = 10 m²), including vertical lines of median (49 m²) and mean (81 m²); D: Extent of black frame within study area showing a sample of mapped shallow landslides.

a gap in the statistical landslide susceptibility and risk literature. In this study, we address this gap by using high resolution data at landscape scale to quantify the reduction in landslide erosion due to individual trees while accounting for local environmental conditions.

Method development for landslide susceptibility modelling is a comprehensive research field that most commonly focuses on generating suitable datasets (e.g., van Westen et al., 2008; Chang et al., 2019; Smith et al., 2021), model development (e.g., Van Den Eeckhaut et al., 2006; Hong et al., 2017; Huang and Zhao, 2018), sampling methods (Heckmann et al., 2014; Conoscenti et al., 2016), model performance and validation (e.g., Rossi et al., 2010; Petschko et al., 2014; Steger et al., 2016a; Xiao et al., 2020), and uncertainty and error evaluation (e.g., Steger et al., 2016b; Steger et al., 2017). All these research objectives have the aim of obtaining reliable landslide susceptibility maps to improve management decisions aimed at reducing landslide risk. We address a knowledge gap related to the integration of individual trees into landslide susceptibility models – specifically for silvopastoral environments. This study is the first of its kind that aims to quantify the reduction in susceptibility to shallow landslide erosion due to the influence of individual trees. We integrate the TIMSS (Spiekermann et al., 2021) of four different tree types for statistical landslide susceptibility assessments using binary logistic regression models. Furthermore, we investigate whether including highly skewed, continuous TIMSS variables in logistic regression modelling has implications for estimation of effect size. Following model development, two farms from the Wairarapa region, New Zealand, are used to illustrate how the landslide susceptibility model can be used to quantify effectiveness of trees for landslide erosion control.

2. Data and methods

2.1. Study area

The study area is an 843 km² area in the Wairarapa in the south-east of the North Island of New Zealand (Fig. 1). Most of the study area (92%) is used for pastoral farming and is underlain by predominantly Neogene-aged massive, poorly bedded mudstone and alternating sandstone and mudstone (Lee and Begg, 2002). Soils commonly have a dense subsoil zone of low permeability formed in loess that is the failure plane for many landslides (De Rose, 2012). A band of coquina limestone forms the central and south-western part of the study area (Fig. 3 in Spiekermann et al., 2021). The terrain has low to moderate relief (<150 m) that is intensely dissected, with narrow ridge and spur crests, hillslopes mostly between 15° and 35°, and narrow valley floors. This topography is locally referred to as “hill country”. Significant areas of colluvium (landslide debris) have accumulated along the base of many hillslopes, and in mid- and upper-slope hollows. Mean annual rainfall is 1100 mm, characterised by winter maxima and summer droughts. Long duration, low intensity rainfall is typical with low daily rainfall totals (De Rose, 2012). However, landslide-generating storms have occurred frequently since climatic records began in the 1880s. Most of these storms do not have particularly high storm or daily rainfall totals (100–200 mm) but often occur when antecedent moisture conditions are high (De Rose, 2012; Basher et al., 2018).

Two farms (Sites 1 and 2) were selected from within the study area in the Wairarapa hill country to quantify the effectiveness of trees on slope stability (Fig. 1). Both farms have a history of landslide and soil erosion research activity (Lambert et al., 1984; De Rose, 2012; Douglas et al., 2013; Basher et al., 2018; Spiekermann et al., 2021). Site 1 is a 1700-ha sheep and beef farm located east of Masterton in a region of steep pastoral hill country. The original native vegetation was cleared between 1860 and 1890 (Lambert et al., 1984). A major rainfall storm event led to widespread landsliding in 1977 (Crozier et al., 1980; Glade, 1998; De Rose, 2012; Fig. 2). Preventative measures were largely non-existent before the event. Soil conservation works in the form of space-planted poplar, willow, and eucalyptus trees began in the

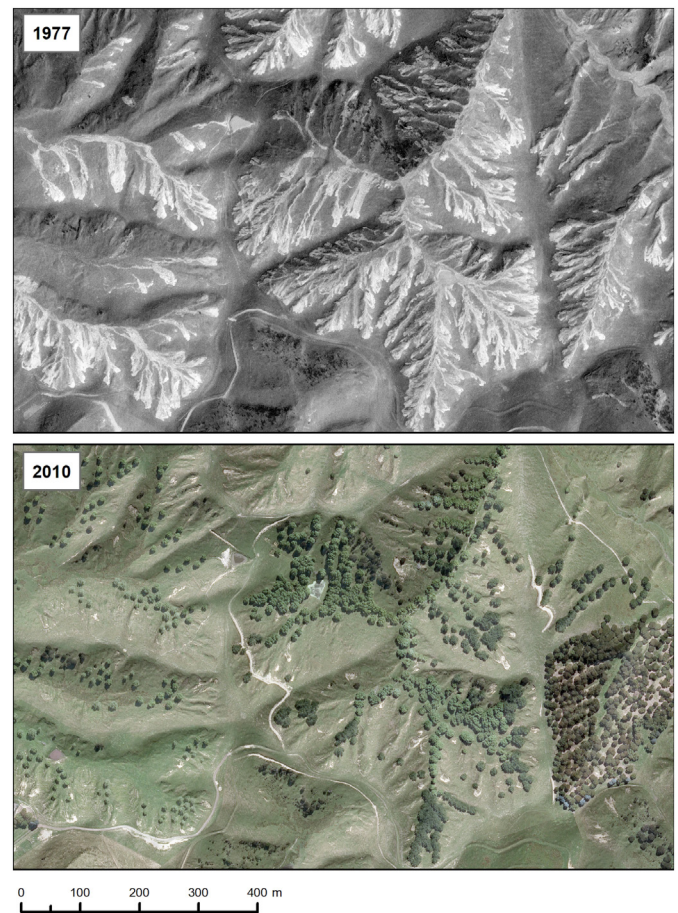


Fig. 2. Susceptibility to landslide erosion is temporally dynamic, as exemplified by a small area within site 1 (see Fig. 1 for location). High density of shallow landslides in 1977 led to extensive space-planting of poplar, willow, and eucalyptus trees (2010).

1980s. While planting has been sustained since commencement, the density of trees on hillslopes differs greatly across the farm, with some hillslopes devoid of tree cover (Table 1). Site 1 is thus representative of a “moderate” level of tree cover for New Zealand’s pastoral hill country farms.

Site 2 is a 462-ha sheep and beef farm located at the upper catchment of the Waikoukou Stream and has had a great deal of soil and water conservation implemented since 1956. The main objectives of these conservation works were to intensively plant slopes and gullies prone to severe erosion using poplars, willows, and protected seedlings of other species. According to farm plan documents (Wairarapa Catchment Board, 1956), the early European land cover likely consisted of light bush, kānuka, and fern, with heavier podocarp species in the wider valleys. Several remnants of kānuka (naturally regenerated following initial clearance) remain distributed across the farm. Overall,

Table 1
Stem counts and densities by tree type at Sites 1 and 2.

Tree type	Site 1			Site 2		
	Count	Percent	Stems per ha	Count	Percent	Stems per ha
Eucalyptus	708	9%	0.4	2247	16%	4.9
Kānuka	1900	25%	1.1	7797	57%	16.9
Conifer	352	5%	0.2	1048	8%	2.3
Poplar/Willow	4545	61%	2.7	2703	20%	5.9
Total	7506	100%	4.4	13,795	100%	29.9

there is a higher tree density (by species and in total) compared with Site 1 (Table 1).

2.2. Landslide inventory

Shallow landslides are the most dominant mass movement process in the study area. This is due to a high-energy geomorphic environment that is predisposed to landsliding with soft sedimentary rocks, steep and highly dissected slopes, and frequent high-intensity rainfall events that regularly trigger many thousands of shallow landslides (Crozier, 2018; Smith et al., 2021). These favourable natural conditions for landslide erosion are compounded by historic changes to land cover with the removal of indigenous forest in the late 1800s to early 1900s for pastoral farming (Glade, 2003). Shallow landslides are commonly small features (50–100 m²; Fig. 1) involving soil and regolith less than 1.5 m deep with long narrow debris tails (Glade, 1998; Crozier, 1996; Basher, 2013; Betts et al., 2017). The triggering mechanism is assumed to be rising pore water pressure due to sustained rainfall reducing the internal friction of soil particles until the gravitational forces ultimately overcome the resistance of the soil.

The landslide inventory used in this study is described by Spiekermann et al. (2021), which we refer to for description of mapping methodology. The shallow landslide dataset consists of 43,069 landslide scars (Fig. 1) that were mapped in regional orthophotos from 2010 (RGB, 0.4 m GSD) and are used in this study to fit and test the landslide susceptibility models. The landslides were triggered by several storms. Two of the storm events, in March 2005 and July 2006, affected the entire study area, with a median recorded rainfall of 175 mm (range: 130–382 mm) and 204 mm (range: 172–321 mm) over 48 and 72 h, respectively. Three further storms, in late July 2006 (149 mm; 48 h), October 2006 (130 mm; 48 h), and June 2009 (197 mm; 24 h), were more localised to the south. The median scar area is 49 m² and the mean is 82.1 m², which is consistent with findings of previous studies (De Rose, 2012; Betts et al., 2017; Smith et al., 2021).

2.3. Predictor variables

To develop the statistical model of landslide susceptibility, key predictor variables of shallow landslide erosion were generated from existing datasets. Selection of predictor variables was based on an understanding of the geomorphic process being assessed, i.e., all selected factors have direct physical process relevance for slope stability. Moreover, since the objective is to investigate the effect of trees on landslide susceptibility, we aimed to keep the model simple by keeping the number of predictor variables to a minimum. Therefore, we include the topographic variables of slope gradient, aspect (northernness, easternness), tree cover using the four TIMSS, and lithology (Table 2).

Slope gradient is the most influential environmental predictor variable used in landslide susceptibility modelling (Carrara et al., 1991,

1995; Chung and Fabbri, 2003; Budimir et al., 2015; Reichenbach et al., 2018) – particularly in combination with variables pertaining to the mechanical properties of soil and lithology (Betts et al., 2017; Reichenbach et al., 2018). The reason for its effective explanatory power is directly related to the physics of mass movement. Slope gradient controls the stresses and resistance acting on a slope to maintain stability (Wu and Sidle, 1995), with increasing shear stress and decreasing resistance for higher slope gradients.

Slope aspect is frequently used as a predisposing factor in landslide susceptibility assessments (e.g., Salter et al., 1983; van Westen et al., 2008; Galli et al., 2008; Ruff and Czurda, 2008). It has been suggested that contrasting microclimate between slopes of different aspect can produce asymmetric valley morphology through control of slope weathering and erosional and depositional processes (Burnett et al., 2008). The direction of incoming weather events may also create a 'shadow effect', impacting some slopes more than others (Liu and Shih, 2013). Crozier et al. (1980) undertook statistical analyses of the distribution of landslides triggered in the winter of 1977 in the Wairarapa and found a strong preference for northerly aspects (61.6% of slips on N, NW, and NE octants). Similarly, another Wairarapa-based study (Gao and Maro, 2010) reports a preference for northerly aspects, which they suggest is a product of deeper weathering from increased solar radiation and wetting and drying cycles experienced by north-facing (southern hemisphere) slopes. Wetting and drying cycles also initiate cracking, resulting in reduced soil cohesion (He et al., 2020) and allowing water to penetrate down to the less permeable bedrock which acts as the surface of rupture (Brooks et al., 2002). The effect of aspect can also be related to structural geology (e.g., dip direction and dip angle of bedding planes; Ruff and Czurda, 2008). Crozier et al. (1980) suggested that preference of landsliding on a particular slope aspect can be temporally dynamic. They found weakest conditions at the bedrock/regolith interface on southerly slopes, and north to west-facing slopes were less disturbed. They therefore postulate that following removal of the original forest cover for pastoral farming, mass movement processes may have initially favoured southern slopes, providing a more extensive, weaker, and undisturbed regolith on north-facing slopes – which was more severely affected in recent times (e.g., the 1977 landslide-triggering rainfall event documented by Crozier et al., 1980 and Gao and Maro, 2010; see Fig. 2). Indeed, landslide susceptibility is not static reality, but is temporally dynamic (Gorsevski et al., 2006; Fig. 2). We therefore include slope aspect in the model to test whether a similar preference can be observed today, or if a change is apparent.

The topographic variables were derived from a 1-m digital elevation model constructed from airborne light detection and ranging (LiDAR) data from 2013. Since the landslides were triggered before the LiDAR surveys, a median filter with 3-m radius was used to remove minor surface roughness produced by the landslide scars to approximate the terrain surface before failure.

Lithology is commonly an important factor in shallow landslide susceptibility modelling since the material type directly influences soil properties such as hydraulic conductivity and texture (Smith et al., 2021). Crozier et al. (1980) found fewer shallow landslides in areas of alluvium, limestone, and sandstone compared with less permeable formations of mudstone and alternating sedimentary rocks. This observation corresponds well to patterns in our landslide inventory (cf. Figs. 1a and 3a), showing a much lower density in limestone terrain. Thus, we hypothesize that lithology is an important predisposing factor. We used lithological data (near-surface rock type) from the NZ Land Resource Inventory, which was derived from 1:250,000 time-stratigraphic geological maps, using stereo aerial photograph interpretation and field verification to aid mapping at a scale of 1:50,000 (Newsome et al., 2008; Fig. 3a). Lithology was converted from vector format to a grid at 1-m GSD. We accept that both boundary and material type errors will result from using lithological data of much lower resolution than for terrain attributes. To ensure sufficient samples were gathered across all material types to safely infer the relationship, we remove material types that are

Table 2

Predictor variables used in landslide susceptibility model [n. = numerical; c. = categorical data]. For lithology, the percentage of study area and number of landslide scars is given for each category.

Data	Model inputs
Topography [n.]	Slope gradient [°]; northernness (cosine transformation of slope aspect), easternness (sine transformation of slope aspect).
TIMSS [n.]	Tree influence models for following vegetation types: eucalyptus, kānuka, conifer, poplar/willow.
Lithology [c.]	Argillite – crushed [0.2%, 48]; Undifferentiated floodplain alluvium [8.5%, 249]; Gravels [0.9%, 229]; Greywacke [1.9%, 178]; Limestone [9.9%, 1252]; Loess [28.7%, 6665]; Mudstone or fine siltstone – banded [6.6%, 4204]; Mudstone or fine siltstone – jointed [19.8%, 15,204]; Mudstone or fine siltstone – massive [15.0%, 10,533]; Sandstone or coarse siltstone – banded [0.1%, 2]; Sandstone or coarse siltstone – massive [8.3%, 4494]; Unconsolidated to moderately consolidated clays [0.2%, 11].

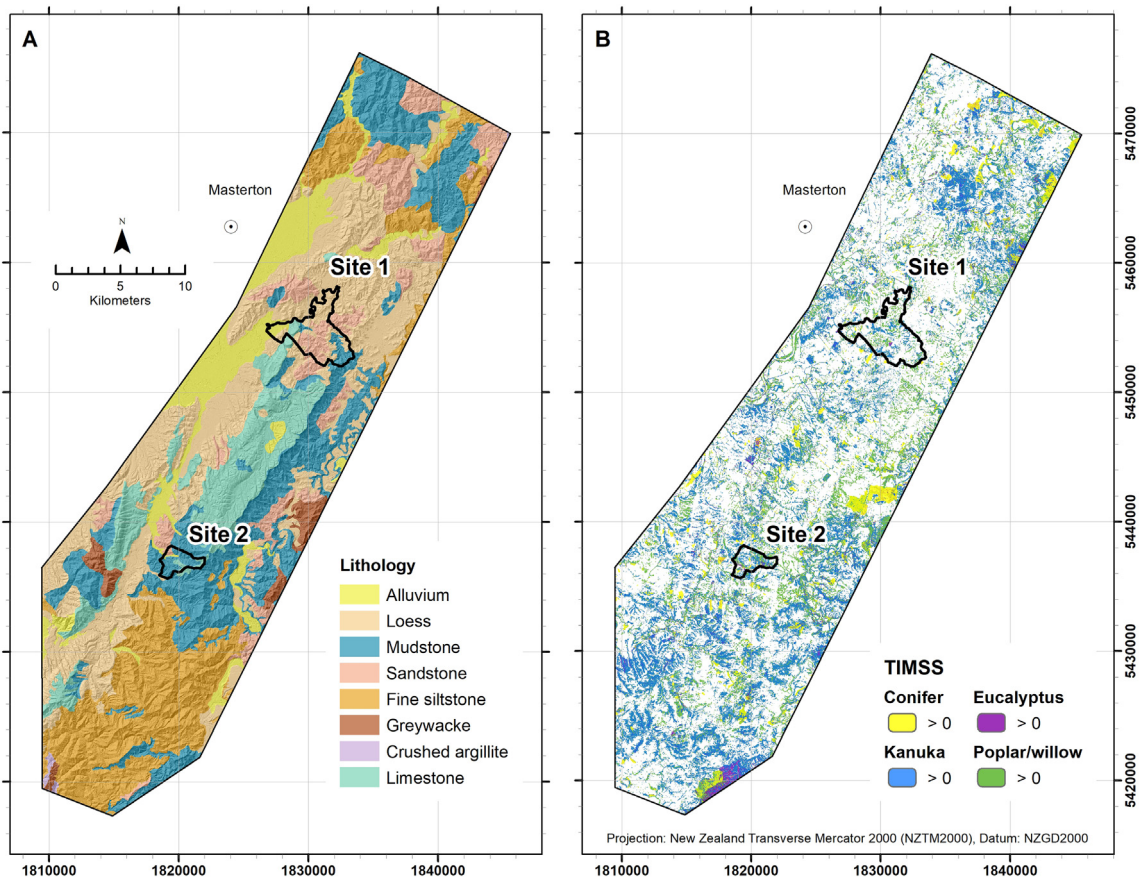


Fig. 3. Insert A: Lithology of study area; Insert B: Tree influence models on slope stability (TIMSS) showing location of different tree types within silvopastoral hill country of study area.

represented in less than 1% of combined presence and absence points (minimum 861 samples of balanced dataset). This led to the removal of four material types: “Argillite – crushed”, “Gravels”, “Sandstone or coarse siltstone – banded”, and “Unconsolidated to moderately consolidated clays” (see Table 2), which reduced the landslide inventory by 290 to 42,778 scars.

Finally, we include the TIMSS (Spiekermann et al., 2021), which we use to quantify the reduction in landslide susceptibility due to the presence of trees in pastoral hill country (Fig. 3b). TIMSS can be defined as spatial representations of the average influence of individual trees on slope stability and were developed for different tree genera based on an empirical relationship between distance from tree and reduction in soil surface eroded. The TIMSS were fit using least-squares logistic regression. Therefore, the models are sigmoidal in shape reaching an asymptotic value denoting the average maximum effective distance of a tree, i.e., the point at which the tree has no observable influence on slope stability due to mechanical and hydrological processes (Schmidt et al., 2001; Istanbuluoglu and Bras, 2005; Phillips and Marden, 2005; Schwarz et al., 2010; Cohen and Schwarz, 2017; Kim et al., 2013; de Jesús Arce-Mojica et al., 2019; Spiekermann et al., 2021). While TIMSS are normalized to 0–1, where 1 is equal to the maximum influence on slope stability of an individual tree of a particular vegetation type, a spatial unit (here, a 1-m pixel) may exceed 1 due to the additive contributions from multiple trees.

TIMSS are available for the dominant tree types in the study area, which include eucalyptus, kānuka, poplar/willow and coniferous tree species. Poplars (*Populus* spp.) and willows (*Salix* spp.) have been a cost-effective option for promoting slope stability in New Zealand’s pastoral hill country. They are easily established from large unrooted poles and rapidly develop extensive root systems (Phillips et al., 2014). Willows and many poplar varieties are tolerant of periodically saturated

soils and have comparatively high transpiration rates during the growing season (Wilkinson, 1999). As with poplars and willows, eucalyptus (*Eucalyptus* spp., e.g., *Eucalyptus globulus*) establish rapidly in cool temperate climates. They are more tolerant to dry soil conditions and summer droughts, but are overall less abundant in the study area (Spiekermann et al., 2021). Unlike poplars and willows, coniferous tree species are mostly found in forestry blocks or used as shelter belts. While the roots of conifers (mostly *Pinus radiata*) are not as strong as kānuka, poplars and willows, they have been shown to root deeply (>2 m) (Watson et al., 1995). Kānuka (*Kunzea* spp.) are commonly found in dense groves and are the most abundant tree species in the study area. As with most indigenous species in New Zealand, kānuka are slower growing, have shallower root systems, but higher tensile strength than exotic species (Watson and Marden, 2004; Phillips et al., 2011). Since many local environmental factors such as soil and climate influence the development of tree root architecture, root systems between and within tree species vary considerably – particularly as a function of plant density as neighbouring plants compete for available resources (nutrients, water, light) (Danjon et al., 2013). However, due to the paucity of species-specific data on root architecture, we use the TIMSS to represent the average influence of an individual tree on slope stability for the four dominant tree types in the study area, assuming an additive function where more than one tree contributes to slope stability at a given point in the landscape. Further details of the development of TIMSS are given in Spiekermann et al. (2021).

2.4. Landslide susceptibility model

2.4.1. Binary logistic regression

We integrate the TIMSS of four different tree types developed by Spiekermann et al. (2021) into a binary logistic regression model

(BLR) to quantify the effectiveness of trees in terms of the reduction in the spatial probability of landslide occurrence. Development of the BLR method is attributed to Cox (1958) and Walker and Duncan (1967) and is the most common statistical method used for landslide susceptibility modelling (Lombardo and Mai, 2018; Reichenbach et al., 2018). It has been shown to produce comparatively low error rates (Brenning, 2005; Smith et al., 2021). We adopt BLR since the effect size of the predictor variables can be quantitatively evaluated using odds ratios. As discussed by Lombardo and Mai (2018), pseudo-quantitative methods that use frequency ratios or expert-knowledge to determine weights for pre-disposing factors (e.g., Persichillo et al., 2017) are not based on underlying probability distributions and are therefore unable to represent the probability of landslide occurrence, which limits the statistical interpretation of the models.

BLR is well suited to landslide susceptibility modelling since it models the probability of a binary response variable ($Y = 0|1$), which corresponds to the absence/presence of landslides. Independent variables can be both numerical and categorical, and as with all regression analyses, the variability of Y is explained in terms of covariates x_1, \dots, x_i . In BLR, the linear function takes on the form:

$$\text{logit}(Y) = \log\left(\frac{p}{1-p}\right) = \beta_0 + \beta_1 x_1 + \dots + \beta_i x_i \tag{1}$$

where y is the dependent variable, i.e., landslide occurrence, x_i is the i -th explanatory variable, β_0 is a constant, β_i is the i -th regression coefficient, and logit is the link function used to convert log-odds ($\pm \infty$) to probability. The logistic function is sigmoidal in shape and always yields values between 0 and 1. The probability of landslide occurrence can thus be formulated as:

$$p(Y = 1) = \frac{1}{1 + \exp^{-(\beta_0 + \beta_1 x_1 + \dots + \beta_i x_i)}} \tag{2}$$

The maximum likelihood estimator is used to fit optimal coefficients for all predictor variables. The maximum likelihood function iteratively fits model coefficients so that p yields values close to 1 where $Y = 1$, and values close to 0 where $Y = 0$ until model convergence is reached. In the context of landslide susceptibility, the probabilities from logistic regression correspond to the predisposition of a given mapping unit to landsliding and are thus often referred to as spatial probabilities with no regard for temporal probability. Logistic regression modelling was performed using the caret package (Kuhn, 2008) within the open-source statistical software R (R Development Core Team, 2021); The raster package was used for model predictions (Hijmans, 2020).

Logistic regression assumes independence of the predictor variables. We used the car package in R (Weisberg and Fox, 2010) to test for multicollinearity by quantifying the variance inflation factor (VIF) for all continuous variables. Variable selection is carried out using a preliminary model with full sample size. A predetermined VIF threshold is commonly used to select variables for removal from the model. While a threshold of 10 is more common (O'Brien, 2007; Heckmann et al., 2014; Smith et al., 2021), we use a more stringent threshold of 2 that has also been used by other authors (e.g., Van Den Eckhaut et al., 2006). Additionally, all variables were removed with a test-statistic for the Wald test (z -statistic) of less than 2, which means the effect size is not significantly different from 0 (95% confidence level) and removal will not significantly affect model fit. All subsequent models use the same variables following removal of insignificant predictor variables.

2.4.2. Sampling design

Landslide susceptibility modelling using logistic regression relies on points in the landscape representing presence and absence of landslides. Though we expect our observations to be correlated, the following steps were taken to increase independence in our observations: each landslide scar was represented by a single centroid pixel (landslide

initiation point – LIP) before extracting spatial data to both landslide presence and absence points. This is a common method aimed at reducing spatial autocorrelation between observations (Atkinson and Massari, 1998; Van Den Eckhaut et al., 2006; Petschko et al., 2014; Lombardo and Mai, 2018). In addition, and before generating absence points, we created a mask to ensure spatial independence of landslides and non-landslides by buffering all landslide polygons by 7.3 m. This distance denotes the 90th percentile of the radius r of the landslide scar inventory, assuming a circular shape. Absence points thus needed to be separated by a distance of $2r$, or 14.5 m. Random absence points were generated in R using the QGIS implementation *qgisprocess* package, an update to the *RQGIS* package (Muenchow et al., 2017).

As noted by Knevels et al. (2020) and Heckmann et al. (2014), the implications of the method used to generate absence points are seldom adequately considered. To evaluate the sensitivity of our model to the selection of absence data, we test the hypothesis that different sampling methods for absence points render significantly different effect sizes for the tree variables. The rationale for doing so is that in silvopastoral landscapes trees are relatively sparsely distributed across the landscape and – by implication – the randomly generated absence points are more likely to fall in open pasture. Since shallow landslides are predominantly triggered in open pasture, the implication is that both presence and absence points mostly have TIMSS values of 0 (Fig. A1; Table 4). Therefore, all four TIMSS variables have very high positive skewness in the distribution of both presence and absence samples (Table 3). While the maximum likelihood estimator is tolerant of highly skewed continuous predictors with large sample sizes, the effect sizes of the variables can be inflated (Alkhalaf and Zumbo, 2017).

The following sampling design is used for presence and absence selection:

- A. *Spatially restricted sampling to twice the effective distance (2xED) of TIMSS:* We created masks at twice the effective distance from trees for each of the TIMSS, which corresponds to 26 m for eucalyptus, 34 m for conifers and kānuka, and 40 m for poplar and willow trees. This has the effect of creating more even spatial odds for presence and random absence points to be located within or beyond the effective distance of trees. This approach reduces the skewness of the TIMSS variables (Table 3). We further hypothesised that this sampling strategy will increase the ability of the maximum likelihood estimator to produce consistent effect sizes. A consequence of masking to 2xED was a reduction in the size of the study area by 45.7% to 458 km². Landslide presence points within 2xED amounted to 26,038. Following Knevels et al. (2020), we randomly generated absence points using a 5:1 absence-presence ratio within the same mask, then resampled $n = 100$ times with a 1:1 landslide presence-absence ratio to account for random variability in the absence samples.

Table 3
Comparison of skewness and sampling frequency of TIMSS variables dependence on sampling strategy (all vs 2xED) using single random selection of absences (1:1).

	Eucalyptus	Kānuka	Poplar/willow	Conifer	All TIMSS
Skewness (1:1 all)	9.9	3.5	2.8	10.0	2.7
Skewness (1:1 2xED)	7.3	2.5	1.9	7.0	1.9
Presence samples >0 (%)	1.1%	10.2%	15.6%	0.5%	16.0%
Absence samples >0 (%)	1.7%	10.8%	16.4%	2.5%	17.6%
Presence and absence >0 (%)	2.8%	21.0%	32.1%	2.5%	33.6%
2xED absence samples >0 (%)	3.3%	18.7%	28.3%	3.9%	30.5%
2xED presence and absence >0 (%)	5.1%	35.5%	54.0%	4.7%	56.9%
Mean (presence >0)	0.29	0.36	0.37	0.34	0.62
Mean (absence >0)	0.45	0.56	0.58	0.77	1.02
Mean (2xED absence >0)	0.47	0.55	0.57	0.77	1.02

- B. *Random sampling across the entire study area (All)*: Absence points were randomly generated to create five times the number of landslide points (213,890). As with sample design A, we resampled $n = 100$ times with a 1:1 landslide presence-absence ratio to produce balanced datasets of 42,778 presence and absence points. To compare like-for-like with sample design A (2xED), we reduced the sample size to 26,038 presence and absence points.
- C. *Combined TIMSS vs class-specific*: To quantify the total effect of trees on landslide susceptibility, the sum of the four TIMSS was included as a single tree factor in separate model runs. This had the effect of reducing the positive skewness associated with the TIMSS of each tree type (Table 3). Effect size and model performance were compared with those of class-specific TIMSS.
- D. *Effect of sample size*: To determine the number of samples required for optimal model performance, we tested model performance for different sample sizes (Heckmann et al., 2014; Petschko et al., 2014; Smith et al., 2021). By reducing the sample size, the average distance between observations increases. This results in greater independence in observations but can come at a cost of not adequately sampling from the diversity of predictor variables in the study area. Small sample sizes lead to greater model variability, which is reversed with increasing sample size. We investigated the point at which spatial autocorrelation was minimized without the cost of poorer model performance. Additionally, we evaluated the effect of sample size on estimation of coefficients and odds ratios. We posit that if effect sizes are not significantly altered with decreasing sample sizes, we may conclude that spatial autocorrelation is not inflating variables when fitting a model using full sample size. We expect model variability to eventually plateau with increasing sample size. The following ten sample sizes were selected: 50, 100, 250, 500, 1000, 2000, 4000, 8000, 16,000, and full sample size of 26,038 presence and absence points. The varied sample sizes were also used to contrast sampling design A (no spatial restrictions), and B (2xED), albeit for a single randomly sampled equal number of absence points.

2.4.3. Model prediction performance

To test model prediction performance of each model, we used k -fold ($k = 5$) cross validation (CV). Samples were randomly partitioned into k folds, whereby $k - 1$ folds are used to train the model and the remaining fold used to test the predictive ability of the model using selected performance measures. This is repeated until each of the five folds has been used for model testing. To ensure the performance measures are not influenced by a particular data partitioning, this process is repeated 10 times. Moreover, we use 100 balanced datasets, each with a different set of randomly selected absence points for 10 repeats of k -fold CV, yielding a total of 5000 coefficient estimates and performance metrics.

Receiver operator curves (ROC) are used to estimate model performance by plotting the true positive rate (sensitivity) against false positive rate ($1 - \text{specificity}$) for each model run across all potential cut-offs. The area under the ROC (AUROC) summarizes a model's prediction performance for balanced samples as it does not depend on the cut-off used to calculate classification accuracy (Hosmer and Lemeshow, 2000). An AUROC score of 1 would mean the model can perfectly discriminate between presence and absence of landslides in its predictions; a value of 0.5 corresponds to no discriminatory power and is equal to that achieved by pure chance. Since a subset of the randomly generated absence points are likely to be located in terrain susceptible to landsliding (i.e., with values similar to those of presence points), an AUC score of 1 is highly unlikely. A good AUC score is considered to be between 0.8 and 0.9; an excellent score is >0.9 (El Khoulou et al., 2009). Model performance metrics and regression coefficients are stored for each of the four sampling methods (A-D). The optimum sampling strategy is determined by comparing performance metrics (median AUROC) and exploring implications for number and density of landslide samples on model variability.

Following selection of the optimal sampling strategy, spatial predictions of susceptibility are made for the two case study sites. The susceptibility values indicate where landsliding can be expected in future, i.e., the values are the probability of belonging to a class associated with unstable terrain (where $Y = 1$). We classified these spatial probabilities of landslide occurrence into three susceptibility classes of low, medium, and high (Petschko et al., 2014; Lombardo and Mai, 2018). The classes correspond to the 5, 20 and, 80 percentiles of the probability distribution extracted at 42,778 LIPs.

2.4.4. Quantifying effectiveness of biological erosion control

As with previous studies that investigated the importance of specific factors in explaining landslide occurrence (Schmaltz et al., 2017; Knevels et al., 2020), we calculated odds ratios (OR) for each of the TIMSS covariates to compare the effectiveness of different tree species in reducing the spatial probability of landslide occurrence. Odds were obtained by exponentiating both sides of Eq. (1) so that:

$$\text{odds} = \frac{p}{1-p} = e^{\beta_0 + \beta_1 x_1 + \dots + \beta_i x_i} \quad (3)$$

Thus, for a unit increase in covariate x_i , the odds of a spatial unit being susceptible to landsliding increase by a factor e^{β_i} , as expressed by odds ratios:

$$\text{OR} = \frac{\text{odds}(x+1)}{\text{odds}(x)} = \frac{e^{\beta_0 + \beta_1 x_1 + \dots + \beta_i (x_i+1)}}{e^{\beta_0 + \beta_1 x_1 + \dots + \beta_i x_i}} = e^{\beta_i} \quad (4)$$

As the TIMSS variables are on the same normalized scale with a value of 1 denoting the maximum tree influence of an individual tree of a vegetation type on slope stability, a direct comparison is possible without rescaling. Besides comparing OR of the four TIMSS variables, we ran predictions for Sites 1 and 2 iteratively dropping a TIMSS variable to explore the impact of the different tree types in reducing landslide susceptibility. We then illustrate how the landslide susceptibility model can be used to quantify the reduction in shallow landslide erosion due to trees present in the landscape.

3. Results

3.1. Variable importance, estimation of effect sizes, and model performance

Multicollinearity tests showed all continuous variables to have a VIF <3 , with the kānuka and poplar/willow TIMSS variables the only factors with a VIF slightly above 2. Thus, all continuous variables were retained in the model. Two lithologies, "Mudstone or fine siltstone – banded" and "Mudstone or fine siltstone – jointed", were removed from the BLR model as the coefficients were not significantly different from 0 and, thus, did not contribute to an improved model fit. Therefore, these two lithologies effectively became the reference category. The remaining six lithologies had coefficients that are significantly less than 0, which means the odds of shallow landsliding are significantly reduced (Table 4). Thus, the most susceptible lithology in the study area are "Mudstone or fine siltstone – banded" and "Mudstone or fine siltstone – jointed", closely followed by "Mudstone or fine siltstone – massive" and "Sandstone/coarse siltstone – massive".

The effectiveness of trees at reducing landslide erosion was quantified using odds ratios, which can be interpreted as factors of change in the odds of a spatial unit being susceptible to shallow landslide erosion. Results show the chosen sampling strategy has very little impact on variation in effect sizes, which is evidenced by minor variations in the odds ratios of the species-specific TIMSS (Fig. 4). Interestingly, the 2xED sampling strategy did not drastically change the effect sizes of TIMSS predictor variables. There is a notable difference in odds ratios of the TIMSS across vegetation types. Sampling from all available presence and absence points (All), median odds ratios for eucalyptus (0.04) and conifer

Table 4

Coefficients, associated standard errors, z-statistics, and odds ratios of predictor variables of final model. p-value of Wald's test and likelihood ratio test < 0.001 for all variables. Note, inputs to the model were not standardized to allow easier interpretation with knowledge of units (Table 1).

Term	β	Std. error	z statistic	OR (95% CI)
(Intercept)	-6.941	0.058	-119.6	
Slope	0.284	0.002	137.2	1.33 (1.32,1.33)
Northernness	0.698	0.017	41.0	2.01 (1.94,2.08)
Easternness	0.209	0.016	13.1	1.23 (1.19,1.27)
Eucalyptus	-3.325	0.159	-20.9	0.04 (0.03,0.05)
Kānuka	-1.228	0.067	-18.2	0.29 (0.26,0.33)
Poplar/Willow	-1.077	0.054	-19.9	0.34 (0.31,0.38)
Conifer	-3.195	0.170	-18.8	0.04 (0.03,0.06)
Alluvium (1 vs 0)	-0.591	0.118	-5.0	0.55 (0.44,0.7)
Greywacke (1 vs 0)	-2.390	0.112	-21.4	0.09 (0.07,0.11)
Limestone (1 vs 0)	-1.261	0.051	-24.5	0.28 (0.26,0.31)
Loess (1 vs 0)	-0.588	0.031	-18.8	0.56 (0.52,0.59)
Mudstone/fine siltstone - massive (1 vs 0)	-0.165	0.030	-5.4	0.85 (0.8,0.9)
Sandstone/coarse siltstone - massive (1 vs 0)	-0.220	0.039	-5.6	0.8 (0.74,0.87)

(0.04) TIMSS were significantly less than that of the poplar/willow (0.33) and kānuka (0.32) TIMSS (Fig. 4). Merging all TIMSS into a single tree variable resulted in a median odds ratio of 0.28 (using unrestricted sampling strategy (*All*)), which is comparable to that of poplar/willow and kānuka. The merged TIMSS also results in less variation in estimation of effect size compared to the species-specific TIMSS. However, results show that both merging TIMSS into a single tree variable and using 2xED sampling led to a reduction in median AUROC (Fig. 5).

As expected, model performance increased greatly with increasing sample size, plateauing above a sample size of 1000 (Fig. 6b, c). The larger range in ROC scores with reduced sample sizes suggests deficient model performance with less than 1000 presence/absence points. While this holds true for both sampling strategies (*All* vs. 2xED), randomly sampling from the entire dataset of presences and absences consistently produced higher median ROC scores and less variance. Odds ratios of the TIMSS fluctuate more with reduced sample sizes and are not

significantly altered with increasing sample sizes beyond 1000 presence/absence points (7a).

The final model used for predictions adopted a sampling strategy using all presence and absence points – again generating 100 balanced sets of all LIPs (42,778) and equal number of absence points, randomly sampled from 5x the number of scars. Again, 5-fold cross-validation using 10 repeats on each of the 100 balanced datasets was used to quantify model performance (Fig. 7). Median AUROC of the 5000 train-test cycles was 0.946, and an IQR of 0.002 (Fig. 7a). The model with the highest median AUROC of the 100 sets was selected for predictions, which had a median AUROC of 0.948 and an accuracy of 88.7% using a cut-off of 0.5 (Fig. 7b). The very low IQR of AUROC suggests model performance is not dependent on the selection of absence points. Variable coefficients and OR of the final model are shown in Table 4. Eucalyptus and conifer TIMSS have the lowest OR at 0.04, followed by kānuka and poplar/willow with 0.29 and 0.34, respectively. The low 95% confidence

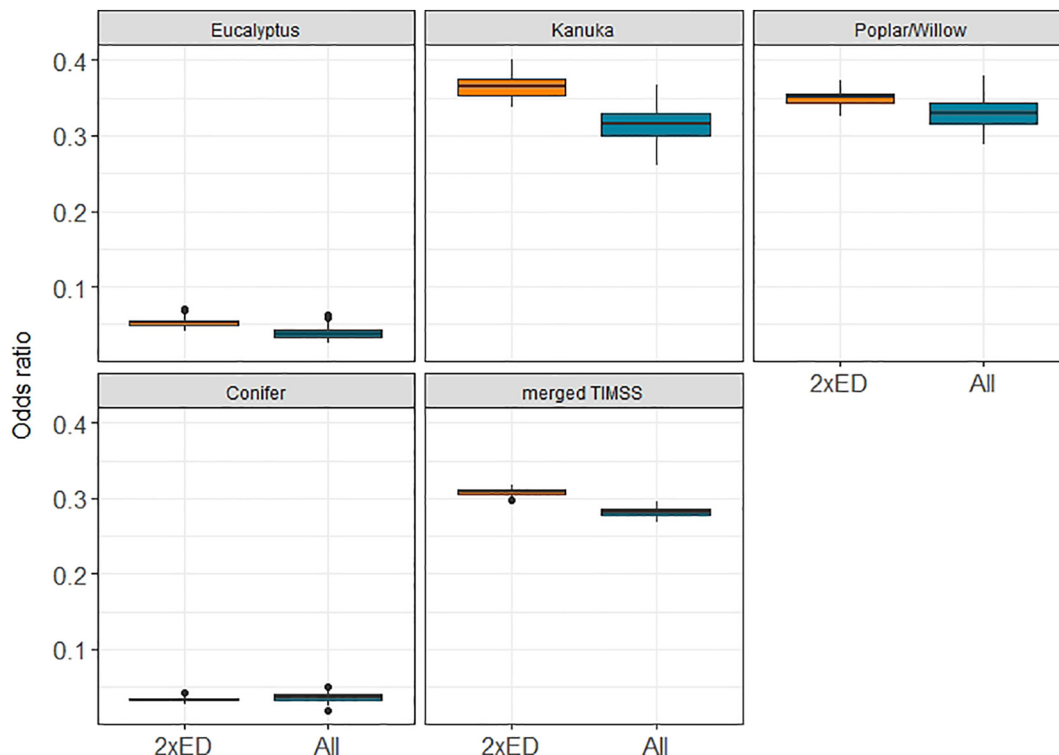


Fig. 4. Comparison of odds ratio of species-specific TIMSS variables and merged TIMSS from 100 BLR models using balanced sample sizes of 26,038 presence and absence points and two different spatial sampling methods (2xED vs *All*).

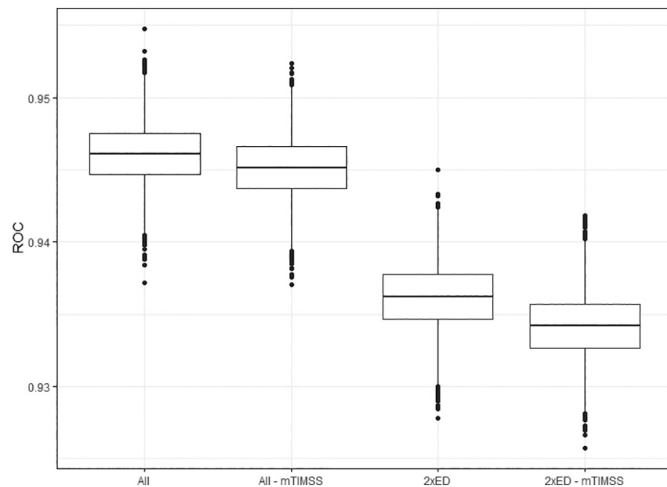


Fig. 5. Boxplots showing AUROC of four different logistic regression models using 10×5 -fold CV with 100 balanced resamples of presence and absence points sampled from: 1) all available landslide presence and absence points; 2) as (1) but with merged TIMSS predictors; 3) landslide presence and absence points within twice the effective distance to trees (2xED); and 4) as (3) but with merged predictors.

intervals indicate high precision of the odds ratios. The spatial distribution of the ORs is shown in Fig. 8.

3.2. Quantifying effectiveness of biological erosion control

For Sites 1 and 2, we illustrate how the landslide susceptibility model can be used to quantify the reduction in landslide erosion due to trees present on the farms. Here, landslide erosion refers to source scar erosion only, not necessarily erosion along the transition zone. We classified the spatial probabilities of the landslide susceptibility map into the three distinct classes based on thresholds related to the percentage of observed landslides falling within each susceptibility class of low (<0.32), medium (0.32 – 0.72) and high (>0.72) corresponding to the 5, 20 and 80 percentiles (Fig. 9). Thus, assuming the same triggering events occur in the future, 80% of landsliding can be expected to be triggered in the “high” class, a further 15% in the “medium” class, and remaining 5% in the “low” class.

Using the final BLR model (Fig. 7b), landslide susceptibility predictions were made for Sites 1 and 2 with and without the TIMSS variables (Fig. 10). Moreover, we iteratively removed a TIMSS variable to explore the impact of the different tree types in reducing landslide susceptibility (Fig. 11).

Sites 1 and 2 have similar distributions of landslide susceptibility across the three classes following removal of tree cover, with 15.0% of Site 1 classified as highly susceptible compared to 14.7% at Site 2 (Fig. 11). Due to current levels of tree cover, the proportion of the sites with highly susceptible land has reduced to 12.1% at Site 1 and 7.3% at Site 2. There is less change in the medium class at Site 1 with a reduction from 17.7% to 16.2%, compared with a reduction from 24.2% to 18.2% at Site 2. At both sites, poplars and willows have contributed most to the reduction, followed by kānuka and eucalyptus. This is not only a function of the abundance, but also due to the efficiency of poplars/willows using wide spacings. While kānuka is the most abundant species in terms of stem count, it is more often concentrated in dense groves. Poplars/willows are distributed more evenly across the susceptibility classes at both sites. This may be because willows are frequently used for riparian planting to stabilize banks in areas of low landslide susceptibility, but it may also indicate a lack of targeted erosion control of highly susceptible slopes. Eucalyptus species at Site 2 are also more efficient than conifers, contributing to an 11% reduction in the high class due to an average density of 5.1 stems/ha. In contrast, kānuka

has reduced susceptibility in the high class by 16.1% due to an average density of 31.1 stems/ha. Thus, wider spacings between trees results in more efficient use of plant material.

Accounting for the rate of landslide erosion across different susceptibility classes (Fig. 9), and assuming the triggering mechanism of observed landslides is the same in the future, landslide erosion has been reduced by 16.6% at Site 1 and 42.9% at Site 2 due to all existing vegetation. While these reductions have been aggregated for each site, the results are scale dependent (e.g., local/paddock vs. farm/catchment). Within each site there is much spatial variation depending on where pre-existing vegetation is located and where plantings have been concentrated in the past.

4. Discussion

4.1. Highly skewed predictor variables for logistic regression

Spatially restricted sampling increased the proportion of both presence and absence points with a TIMSS value >0 – in all cases reducing the positive skew (Table 3). However, due to the difference in abundance across the tree classes within the study area, the positive skewness remained high for both eucalyptus (9.9 down to 7.3) and conifer (10.0 to 7.0) compared with kānuka (3.5 to 2.5) and poplar/willow TIMSS (2.8 to 1.9). This is simply a reflection of the proportion of samples in proximity to conifers and eucalyptus species in the study area (for species abundance see Spiekermann et al., 2021). Since the positive skewness associated with eucalyptus and conifer TIMSS remains high regardless of sampling strategy used, the risk of inflated effect size is not significantly reduced. Yet, Alkhalaf and Zumbo (2017) found that highly skewed continuous predictors are only problematic when sample sizes are small. Given that we use very large sample sizes (total of 85,556 using all LIPs and equal number of absence points), we can assume that the highly skewed eucalyptus and conifer TIMSS predictors will not affect the estimation and inferences.

However, we further tested this by creating domain-specific models by iteratively sampling presence and absence points according to tree type, i.e., restricting sample selection to 2xED of the conifer class, followed by eucalyptus class. This significantly reduced the sample size (conifer domain: 1477 LIPs; eucalyptus domain: 3092), but also reduced the positive skewness (conifer domain 2.15; eucalyptus domain 2.49). Interestingly, the estimate of effect size was not significantly altered due to the reduction in positive skewness (OR: conifer TIMSS 0.07; eucalyptus TIMSS 0.09). Thus, we conclude that the estimates produced using all available LIPs are valid and robust.

4.2. Effect sizes and model performance

In terms of differences in effect size, the BLR found a notable difference in OR across tree type, including the spatial distribution surrounding trees (Table 4; Fig. 8). In particular, the lower odds in landslide occurrence associated with *Pinus radiata* contradict knowledge of the root strengths of these species. Watson and Marden (2004) found mean live-root tensile strengths for *Pinus radiata* to be only 40% and 50% of kānuka and ‘Veronese’ poplar (*Populus deltoides x nigra*) root strengths, respectively. In part, this apparent discrepancy may be explained by the greater density of planted conifers compared with poplar/willows and may also be due to differences in age distributions. Furthermore, a value of 1 in the conifer and kānuka TIMSS corresponds to the influence of approximately 3 stems on average, since these species are more difficult to delineate, given crown morphology and tree density (see Spiekermann et al., 2021). However, some uncertainty and error from the landslide mapping and species classification will be propagated through to the measure of effect size for different tree types. We note that in the process of mapping landslides, scars (or portions thereof) may have been obscured by the canopy cover. This source of error may lead to an overestimation of effect size of trees, which

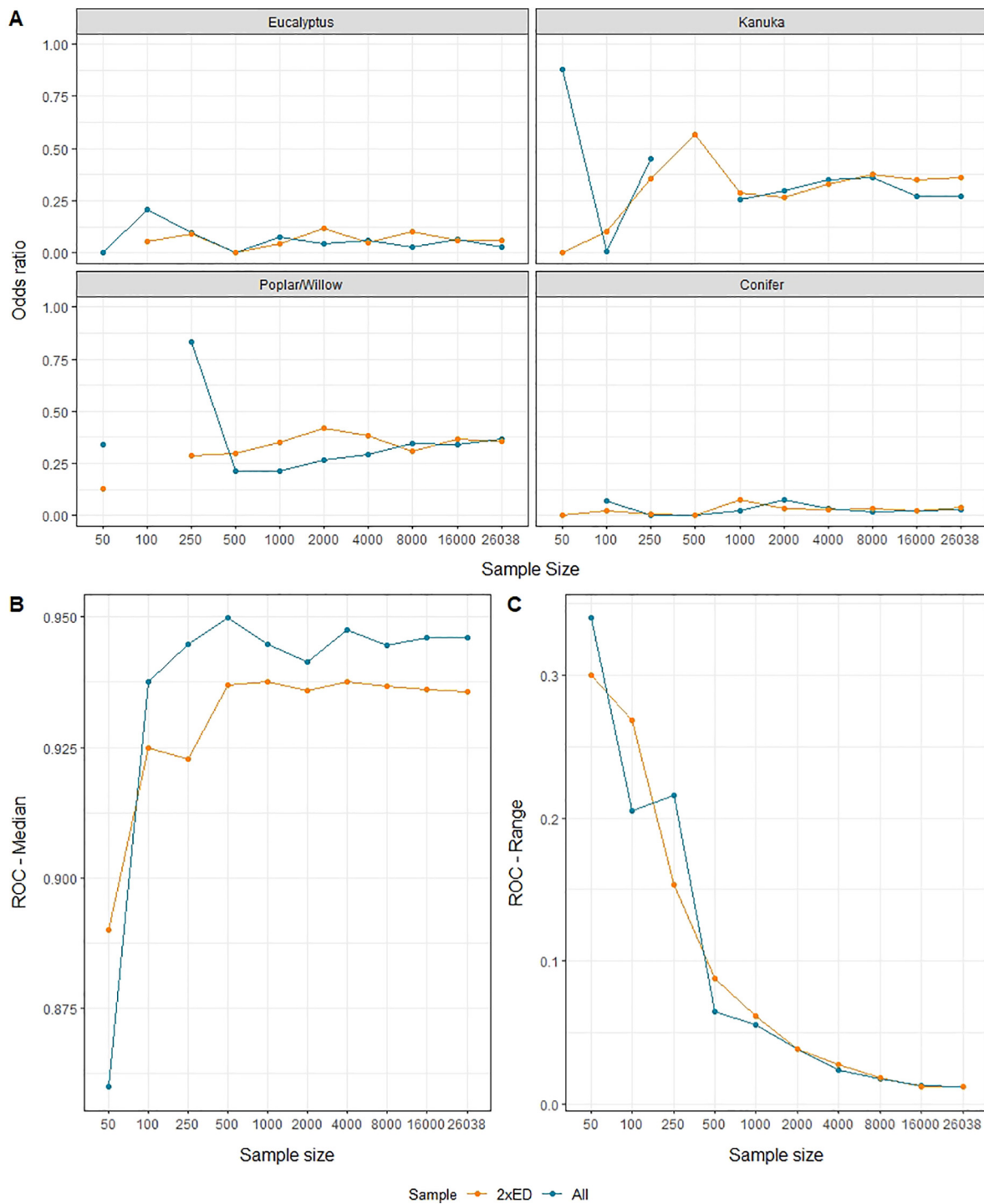


Fig. 6. A) Dependence of odds ratio of TIMSS variables on sample size; Data gaps are values >1. B) and C) Area under ROC (median, range) with increasing sample size, contrasting sampling strategies based on single random sample and 20 × 5-fold CV.

would likely be more pronounced for smaller landslide inventories. Additionally, the influence of trees on slope stability is dependent on the age of the tree and the extent of the root systems. This study uses a fixed representation of tree influence on slope stability for four tree types, which does not change as a function of allometric relationships to above-ground metrics such as tree height.

To determine whether spatial autocorrelation was present and resulting in inflated effect sizes of the TIMSS variables, we compared resulting ORs based on nine different sample sizes (100–26,038). With samples >1000 presence and absence points, estimates became

relatively stable while the range in AUROC of repeated train-tests using cross-validation dropped below 0.1 (Fig. 6C). Since estimates of effect sizes were not significantly altered with smaller sample sizes, we may conclude that spatial autocorrelation is not inflating variables when fitting models using the full sample size. Furthermore, including all available data to train the model results in an improvement in model performance without affecting statistical inferences.

The performance of the final model has an AUROC of 0.95, which equates to an accuracy of 88.7% using a cut-off of 0.5 for binary classification (Fig. 7B). Given the relatively simple model with few predictor

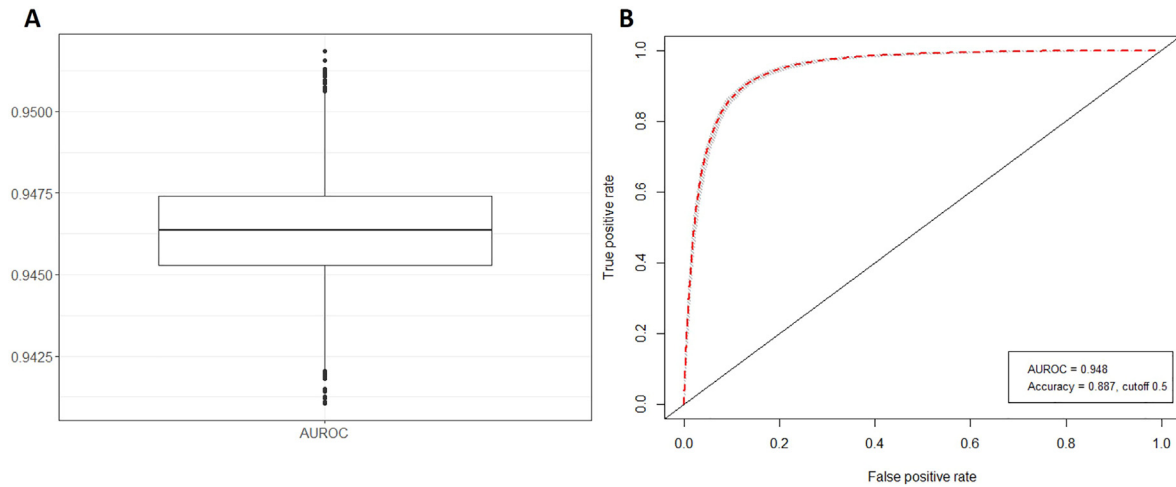


Fig. 7. A: Boxplot of AUROC based on 100 balanced sets of all landslide scars (42,778) and equal number of randomly selected absence points, each using 10×5 -fold cross-validation (total of 5000 resamples). Best of the 100 final models was selected using greatest median AUROC score for predictions. B: The ROC of the final model selected for predictions – ROC of 50 folds (grey), final model (red dash; AUROC 0.948).

variables, a comparably high AUROC score was achieved, which is not uncommon when LiDAR data are used for detailed topographic representation (e.g., Petschko et al., 2014; Knevels et al., 2020). The detailed representation of land cover through integration of individual trees improved model performance – albeit subtle with an increase in AUROC from 0.937 to 0.948. Thus, models with different predictor variables can be similar in terms of their performance, but the implications can be significant for the geomorphic plausibility of spatial predictions and land management decisions (Steger et al., 2016a).

Further improvements in performance by including additional predictor variables (e.g., curvature or surface roughness) are likely to be incremental, since a proportion of randomly generated absence points will always be located on slopes susceptible to landslide erosion. In our two case studies, these highly susceptible areas equated to approximately 7.3% and 12.1% (Fig. 11). Sensitivity using the final model was calculated to be 0.859, and specificity 0.903, which means the rate of false positives was lower than that of false negatives. Therefore, false positives are inherently unavoidable using this method to create absences for binary logistic regression.

Besides the TIMSS variables, the topographic and lithology predictors are important factors to consider. Slope gradient has an OR of 1.33, which means that for an increase in 1 degree, the odds of landslide occurrence increase by a factor of 1.33, and since the increase is exponential, an increase of 10 degrees increases the odds by a factor of 17.06. Northern aspect doubles the odds of landsliding compared with southern aspect, whereas an east-west gradient was less important, though landslide susceptibility increases slightly on eastern aspects (Table 3). In terms of lithology, greywacke and limestone are the least susceptible lithologies with ORs of 0.09 and 0.28, respectively. These ORs are to be interpreted with reference to the two reference lithologies “Mudstone or fine siltstone – banded” and “Mudstone or fine siltstone – jointed”, i.e., with all else equal, the odds of landsliding on limestone are a tenth of that on mudstone.

Statistical models have previously been used to evaluate variable importance and effect sizes of differing land covers to explain landslide occurrence, albeit not at the level of individual trees. For example, Knevels et al. (2020) examined differences across LULC classes. The authors found broad-leaf and mixed forests were less susceptible to landslides than conifer forests. Moreover, forests were in general far less likely to

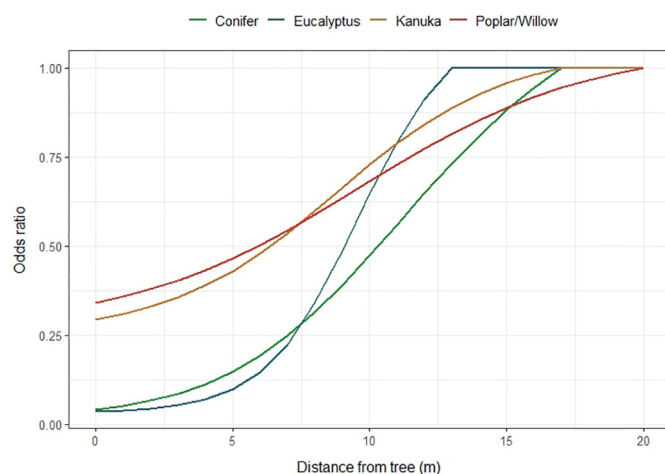


Fig. 8. Spatial distribution of odds ratio for each tree type as a function of distance from tree. Odds ratios are calculated using the exponential function of the regression coefficient multiplied with the TIMSS values at increasing distance from a tree. An odds ratio of 1 means there is no change to outcome (= maximum effective distance of an individual tree), and an odds ratio less than 1 is associated with lower odds of outcome.

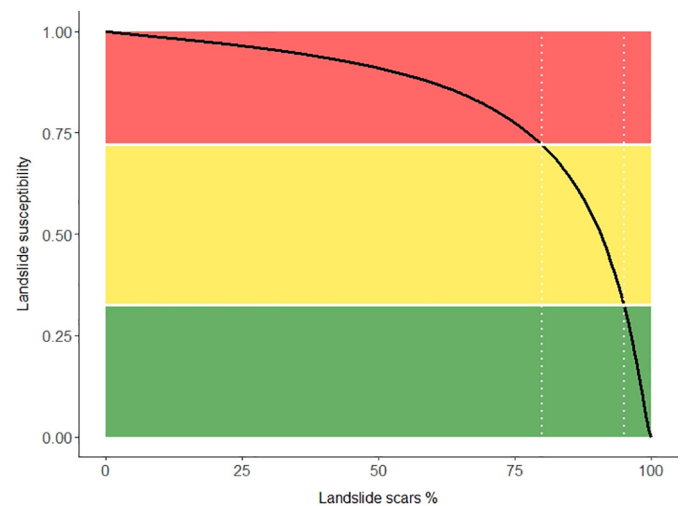


Fig. 9. Cumulative percentage of landslide scars in three susceptibility classes defined according to 5, 20, and 80 percentiles of probability values at landslide initiation points. The class thresholds correspond to probability values of 0.32, and 0.72.

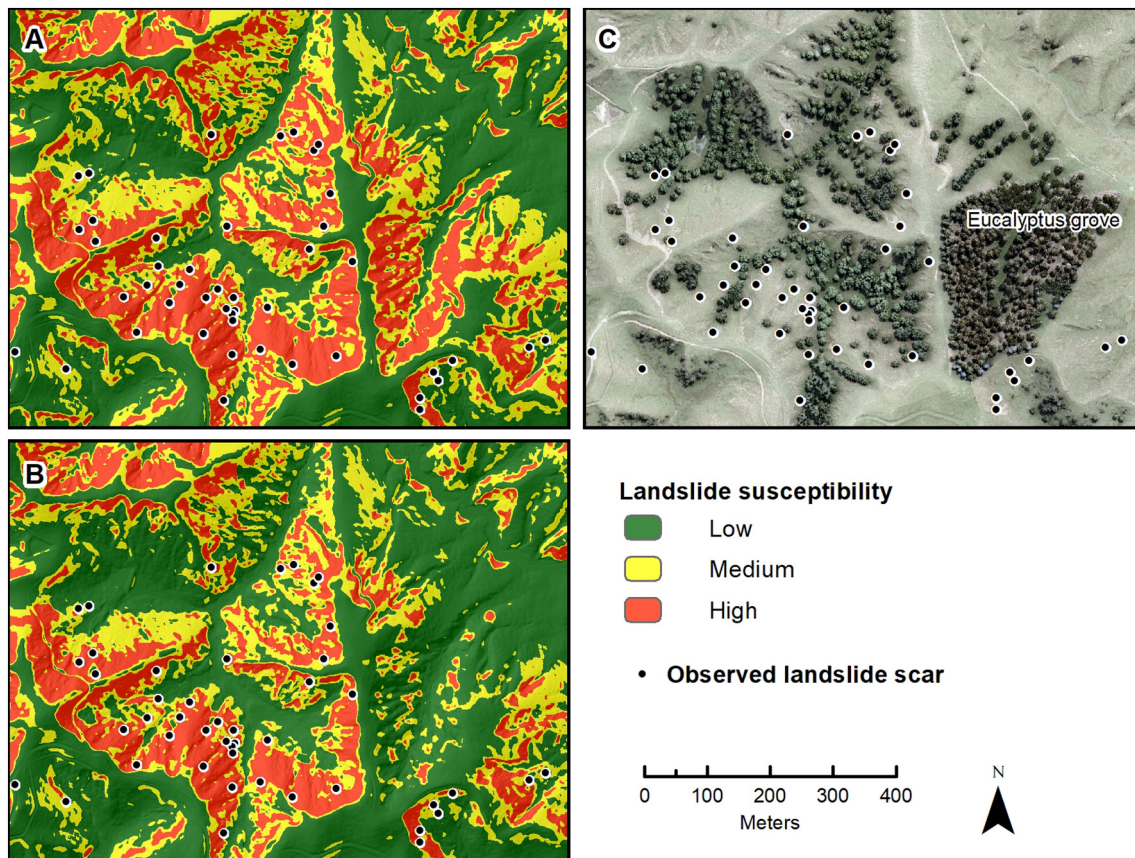


Fig. 10. Landslide susceptibility for a small area within Site 1: A) Landslide susceptibility with no trees; B) Landslide susceptibility with trees present in 2013; C) distribution of trees – mainly poplars/willows, and eucalyptus species. Note, the eucalyptus grove in the southeast of insert C has led to a much greater reduction in landslide susceptibility compared with the poplars and willows to the west, which were largely planted in areas of low susceptibility.

experience landsliding compared to non-forested areas (odds ratio of 0.03). A similar forest effect, albeit of lower magnitude (odds ratio of 0.21) has been found elsewhere (Schmaltz et al., 2017). These results are supported by many additional studies that found substantial differences in landslide occurrence across different land cover classes (Glade, 1998, 2003; Song et al., 2008; Basher, 2013; Marden et al., 2014; Papathoma-Köhle and Glade, 2013; Phillips et al., 2018). Persichillo et al. (2017) investigated the effect of land use changes on the occurrence of shallow landslides using multi-temporal land-use maps. Other studies have combined assessments of historic land cover dynamics to inform future scenarios (Reichenbach et al., 2014; Pisano et al., 2017; Torizin et al., 2018). Concluding that land cover significantly alters landslide risk, they encourage the use of multi-temporal landslide inventories aligned with concurrent LULC data. Indeed, landslide susceptibility is no static reality, but is temporally dynamic (Gorsevski et al., 2006).

4.3. Implications for land management

The landslide susceptibility model developed here can be used to improve targeting of erosion mitigation measures. An interesting observation from the case studies is that landsliding is highly concentrated to certain areas of the landscape. Indeed, 80% of future landsliding is predicted to be found within 12.1% (206 ha) and 7.3% (34 ha) of Sites 1 and 2, respectively (Fig. 11). This points towards the potential for smarter targeting of erosion control. Conversely, implementing tree planting in less susceptible terrain (e.g., the medium class) will not be as efficient in terms of reduction in landslide erosion on a per tree basis since only 15% of landslides are expected to occur in terrain of medium susceptibility. Yet, the feasibility of treatment is likely to be

reduced in areas of high susceptibility due to unfavourable conditions for plant growth (e.g., shallow soils, increased moisture stress, exposure to wind gusts, etc.).

Recently, national-scale assessments aimed at quantifying on-farm mitigation in New Zealand assumed a 70% reduction in sediment yield across all farms that had a farm environmental plan involving widely spaced plantings of trees (Neverman et al., 2019; Monaghan et al., 2021) – which assumes space planting of all slopes (Hawley and Dymond, 1988). Such assumptions are commonly used in models to inform policy development at regional to national scale (Basher et al., 2020; McDowell et al., 2020; Monaghan et al., 2021). Using high resolution data, this study, while limited to two farms, has undertaken a spatially explicit quantification of the reduction in landslide erosion due to trees actually present in the landscape. Both farms have a history in soil conservation – Site 1 since the 1980s, Site 2 since the 1950s. The results shed some doubt on the previously assumed effectiveness of tree planting in the context of farm environment plans, since mitigation effectiveness is very much dependent on the scale of plantings (both number and density) and the targeting of susceptible land. In the absence of spatially explicit assessments that evaluate the reduction in landsliding due to actual mitigation measures, the assumptions made by such national-scaled models may provide misleading expectations to policy planners and practitioners alike when not interpreted with good knowledge of the assumptions.

5. Conclusion

We developed a landslide susceptibility model using binary logistic regression for silvopastoral landscapes. For the first time, the influence of individual trees of different vegetation types is integrated into a

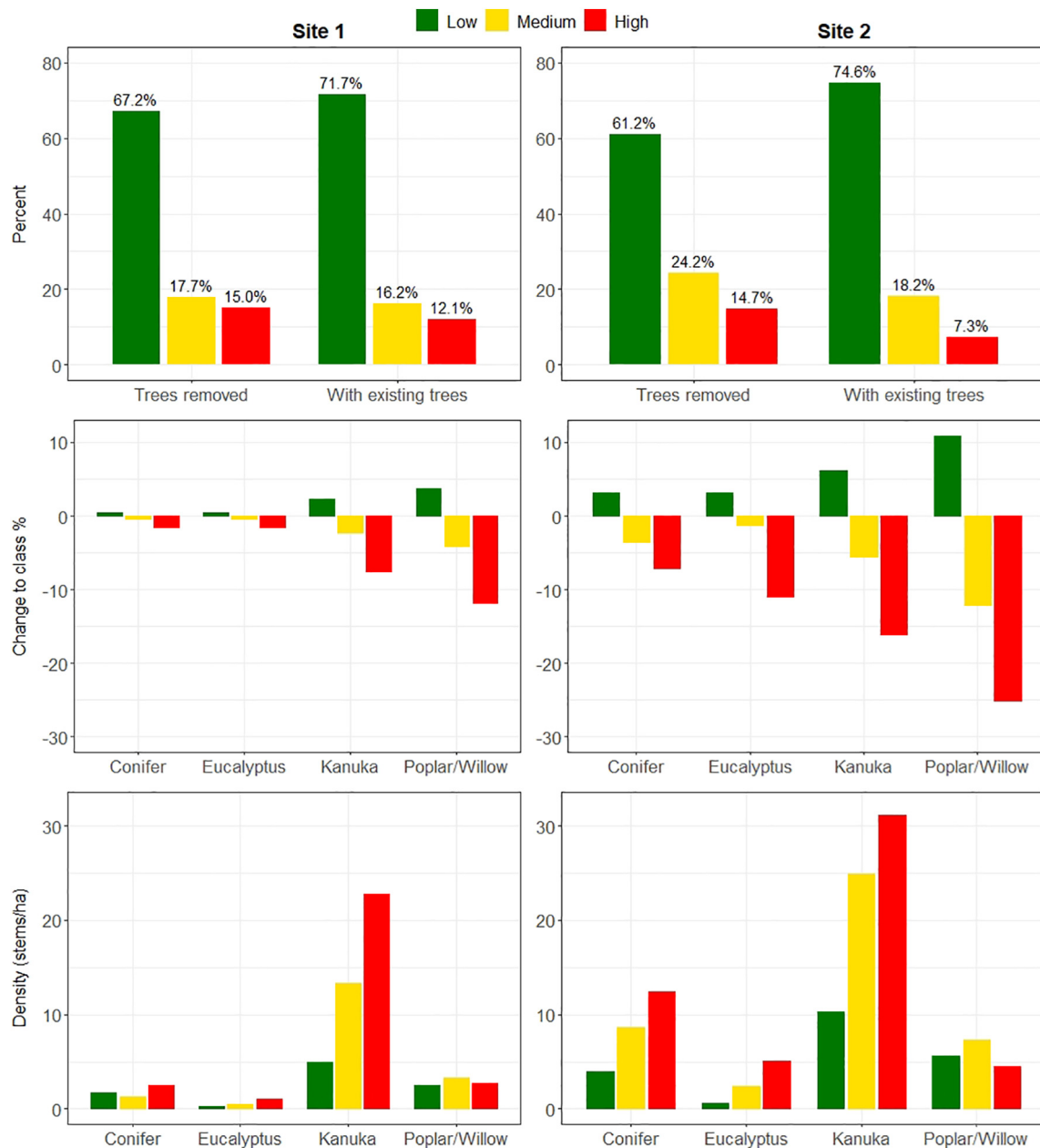


Fig. 11. For Sites 1 (left column) and 2 (right column): percentage of landslide susceptibility classes (low, medium, and high) with and without trees; contribution of different tree types to change (%) in landslide susceptibility; density (stems/ha) of different species across susceptibility classes.

statistical landslide susceptibility model. Model performance was very good, with a median AUROC of 0.95 in the final model used for predictions, which equates to an accuracy of 88.7%. The effect of highly skewed continuous variables on the maximum likelihood estimator was investigated by testing different sampling strategies aimed at reducing positive skewness. With an adequate sample size, we found that highly skewed continuous predictor variables do not result in an inflation of effect size.

The effectiveness of trees at reducing landslide erosion was quantified using odds ratios, which can be interpreted as factors of change in the odds of a spatial unit being susceptible to shallow landslide erosion. The odds ratio for poplar/willow trees indicated that the odds of shallow landslides were reduced by a factor of 0.34 close to the base of poplar/willow trees, whereas at a distance of 20 m from the tree, the average tree had no measurable effect on landslide susceptibility. Eucalyptus had a lower odds ratio (greater effect) at close proximity with an OR of 0.04 at tree stem, but reaching an odds ratio of 1 at 13 m. Kānuka

had a similar spatial pattern to poplar/willows, but is more difficult to interpret as individual trees are more difficult to delineate, which means the effect is a function of multiple stems (approximately 3 stems).

We illustrated application of the landslide susceptibility model by quantifying the reduction in shallow landslide erosion due to trees, for two case study sites, and also evaluated reductions achieved by tree type. Future landslide erosion was reduced by 16.6% at Site 1 and 42.9% at Site 2 due to all existing vegetation. The effectiveness of individual trees on reducing landslide erosion was shown to be less a function of species than that of targeting highly susceptible areas with adequate plant densities. We found 80% of landslides are triggered in 12.1% and 7.3% of Sites 1 and 2, respectively, suggesting there is great potential for smarter targeting of erosion control by decision-makers in land management. The high-resolution spatial information provided by the landslide susceptibility map can be used to support the development of landslide erosion mitigation measures.

Supplementary data to this article can be found online at <https://doi.org/10.1016/j.geomorph.2021.107993>.

Declaration of competing interest

The authors declare that they have no known competing financial interests or personal relationships that could have appeared to influence the work reported in this paper.

Acknowledgements

This research was supported by New Zealand Ministry of Business, Innovation and Employment research program “Smarter Targeting of Erosion Control (STEC)” (Contract C09X1804) and the Strategic Science Investment Fund (SSIF) allocated to Landcare Research. Special thanks to Dr. Chris Phillips and Dr. Les Basher for reviewing the manuscript prior to submission.

References

- Alkhalaf, A., Zumbo, B.D., 2017. The impact of predictor variable(s) with skewed cell probabilities on Wald tests in binary logistic regression. *J. Mod. Appl. Stat. Methods* 16, 40–80. <https://doi.org/10.22237/jmasm/1509494640>.
- Atkinson, P.M., Massari, R., 1998. Generalised linear modelling of susceptibility to landsliding in the central Apennines. *Comput. Geosci.* 24, 373–385.
- Basher, L.R., 2013. *Erosion Processes and their Control in New Zealand*. *Ecosyst. Serv. N. Z. Cond. Trends* 363–374.
- Basher, L., Betts, H., Lynn, I., Marden, M., McNeill, S., Page, M., Rosser, B., 2018. A preliminary assessment of the impact of landslide, earthflow, and gully erosion on soil carbon stocks in New Zealand. *Geomorphology* 307, 93–106. <https://doi.org/10.1016/j.geomorph.2017.10.006>.
- Basher, L., Spiekermann, R., Dymond, J., Herzog, A., Hayman, E., Ausseil, A.G., 2020. Modelling the effect of land management interventions and climate change on sediment loads in the Manawatū-Whanganui region. *N. Z. J. Mar. Freshw. Res.* 54, 490–511. <https://doi.org/10.1080/00288330.2020.1730413>.
- Betts, H., Basher, L., Dymond, J., Herzog, A., Marden, M., Phillips, C., 2017. Development of a landslide component for a sediment budget model. *Environ. Model. Softw.* 92, 28–39. <https://doi.org/10.1016/j.envsoft.2017.02.003>.
- Brabb, E.E., 1984. Innovative approaches to landslide hazard mapping. 4th International Symposium on Landslides. 16–21 September 1984, Toronto, Canada, pp. 307–324.
- Brandt, M., Tucker, C.J., Kariryaa, A., Rasmussen, K., Abel, C., Small, J., Chave, J., Rasmussen, L.V., Hiernaux, P., Diouf, A.A., Kergoat, L., Mertz, O., Igel, C., Gieseke, F., Schöning, J., Li, S., Melocik, K., Meyer, J., Sinno, S., Romero, E., Glennie, E., Montagu, A., Dendoncker, M., Fensholt, R., 2020. An unexpectedly large count of trees in the West African Sahara and Sahel. *Nature* 587, 78–82. <https://doi.org/10.1038/s41586-020-2824-5>.
- Brenning, A., 2005. Spatial prediction models for landslide hazards: Review, comparison and evaluation. *Nat. Hazards Earth Syst. Sci.* 5, 853–862. <https://doi.org/10.5194/nhess-5-853-2005>.
- Brooks, S.M., Crozier, M.J., Preston, N.J., Anderson, M.G., 2002. Regolith stripping and the control of shallow translational hillslope failure: Application of a two-dimensional coupled soil hydrology-slope stability model, Hawke's Bay, New Zealand. *Geomorphology* 45, 165–179. [https://doi.org/10.1016/S0169-555X\(01\)00153-2](https://doi.org/10.1016/S0169-555X(01)00153-2).
- Budimir, M.E.A., Atkinson, P.M., Lewis, H.G., 2015. A systematic review of landslide probability mapping using logistic regression. *Landslides* 12, 419–436. <https://doi.org/10.1007/s10346-014-0550-5>.
- Burnett, B.N., Meyer, G.A., McFadden, L.D., 2008. Aspect-related microclimatic influences on slope forms and processes northeastern Arizona. *J. Geophys. Res. Earth Surf.* 113, 1–18. <https://doi.org/10.1029/2007JF000789>.
- Carrara, A., Cardinali, M., Detti, R., Guzzetti, F., Pasqui, V., Reichenbach, P., 1991. GIS techniques and statistical models in evaluating landslide hazard. *Earth Surf. Proc. Land.* 16, 427–445. <https://doi.org/10.1002/esp.3290160505>.
- Carrara, A., Cardinali, M., Guzzetti, F., Reichenbach, P., 1995. GIS technology in mapping landslide hazard. In: Carrara, A., Guzzetti, F. (Eds.), *Geographical Information Systems in Assessing Natural Hazards*. Kluwer Academic Publisher, Dordrecht, The Netherlands, pp. 135–176.
- Cervi, F., Berti, M., Borgatti, L., Ronchetti, F., Manenti, F., Corsini, A., 2010. Comparing predictive capability of statistical and deterministic methods for landslide susceptibility mapping: a case study in the northern Apennines (Reggio Emilia Province, Italy). *Landslides* 7, 433–444. <https://doi.org/10.1007/s10346-010-0207-y>.
- Chang, K.T., Merghadi, A., Yunus, A.P., Pham, B.T., Dou, J., 2019. Evaluating scale effects of topographic variables in landslide susceptibility models using GIS-based machine learning techniques. *Sci. Rep.* 9, 1–21. <https://doi.org/10.1038/s41598-019-48773-2>.
- Chung, C.J.F., Fabbri, A.G., 2003. Validation of spatial prediction models for landslide hazard mapping. *Nat. Hazards* 30, 451–472. <https://doi.org/10.1023/B:NHAZ.0000007172.62651.2b>.
- Cislaghi, A., Chiaradia, E.A., Bischetti, G.B., 2017. Including root reinforcement variability in a probabilistic 3D stability model. *Earth Surf. Process. Landforms* 42, 1789–1806. <https://doi.org/10.1002/esp.4127>.
- Cohen, D., Schwarz, M., 2017. Tree-root control of shallow landslides. *Earth Surf. Dyn.* 5, 451–477. <https://doi.org/10.5194/esurf-5-451-2017>.
- Conoscenti, C., Rotigliano, E., Cama, M., Caraballo-Arias, N.A., Lombardo, L., Agnesi, V., 2016. Exploring the effect of absence selection on landslide susceptibility models: a case study in Sicily, Italy. *Geomorphology* 261, 222–235. <https://doi.org/10.1016/j.geomorph.2016.03.006>.
- Cox, D.R., 1958. The regression analysis of binary sequences. *J. R. Stat. Soc. Ser. B* 20, 215–232. <https://doi.org/10.1111/j.2517-6161.1958.tb00292.x>.
- Crozier, M.J., 1996. Runout behaviour of shallow, rapid earthflows. *Zeitschrift Für Geomorphol. Suppl.* 35–48.
- Crozier, M.J., 2018. Reprint of “a proposed cell model for multiple-occurrence regional landslide events: implications for landslide susceptibility mapping”. *Geomorphology* 307, 3–11. <https://doi.org/10.1016/j.geomorph.2018.02.001>.
- Crozier, M.J., Eyles, R.J., Crozier, M.J., McConchie, J.A., Owen, R.C., 1980. Distribution of landslides in the Wairarapa hill country. *N. Z. J. Geol. Geophys.* 23, 575–586. <https://doi.org/10.1080/00288306.1980.10424129>.
- Danjon, F., Stokes, A., Bakker, M.R., 2013. Root systems of woody plants. *Plant Roots Hidden Half*, Fourth ed., pp. 431–456.
- de Jesús Arce-Mojica, T., Nehren, U., Sudmeier-Rieux, K., Miranda, P.J., Anhof, D., 2019. Nature-based solutions (NbS) for reducing the risk of shallow landslides: where do we stand? *Int. J. Disaster Risk Reduct.* 41. <https://doi.org/10.1016/j.ijdrr.2019.101293>.
- De Rose, R.C., 2012. Slope control on the frequency distribution of shallow landslides and associated soil properties, North Island, N. Z. *Earth Surf. Process. Landforms* 38, 356–371. <https://doi.org/10.1002/esp.3283>.
- Douglas, G.B., McIvor, I.R., Manderson, A.K., Todd, M., Braaksma, S., Gray, R.A.J., 2009. Effectiveness of space-planted trees for controlling soil slippage on pastoral hill country. In: Currie, L.D., Lindsay, C.L. (Eds.), *Nutrient management in a rapidly changing world*. Massey University, Occasional Report No. 22. Palmerston North, Fertilizer and Lime Research Centre.
- Douglas, G.B., McIvor, I.R., Manderson, A.K., Koolaard, J.P., Todd, M., Braaksma, S., Gray, R.A.J., 2013. Reducing shallow landslide occurrence in pastoral hill country using wide-spaced trees. *Land Degrad. Dev.* 24, 103–114. <https://doi.org/10.1002/ldr.1106>.
- El Khouli, R.H., Macura, K.J., Barker, P.B., Habba, M.R., Jacobs, M.A., Bluemke, D.A., 2009. Relationship of temporal resolution to diagnostic performance for dynamic contrast enhanced MRI of the breast. *J. Magn. Reson. Imaging* 30, 999–1004. <https://doi.org/10.1002/jmri.21947>.
- Galli, M., Ardizzone, F., Cardinali, M., Guzzetti, F., Reichenbach, P., 2008. Comparing landslide inventory maps. *Geomorphology* 94, 268–289. <https://doi.org/10.1016/j.geomorph.2006.09.023>.
- Gao, J., Maro, J., 2010. Topographic controls on evolution of shallow landslides in pastoral Wairarapa, New Zealand, 1979–2003. *Geomorphology* 114, 373–381. <https://doi.org/10.1016/j.geomorph.2009.08.002>.
- Glade, Thomas, 1998. Establishing the frequency and magnitude of landslide-triggering rainstorm events in New Zealand. *Environ. Geol.* 35, 160–174.
- Glade, T., 2003. Landslide occurrence as a response to land use change: a review of evidence from New Zealand. *Catena* 51, 297–314. [https://doi.org/10.1016/S0341-8162\(02\)00170-4](https://doi.org/10.1016/S0341-8162(02)00170-4).
- Gómez, C., White, J.C., Wulder, M.A., 2016. Optical remotely sensed time series data for land cover classification: a review. *ISPRS J. Photogramm. Remote Sens.* 116, 55–72. <https://doi.org/10.1016/j.isprsjprs.2016.03.008>.
- Gorsevski, P.V., Gessler, P.E., Boll, J., Elliot, W.J., Foltz, R.B., 2006. Spatially and temporally distributed modeling of landslide susceptibility. *Geomorphology* 80, 178–198. <https://doi.org/10.1016/j.geomorph.2006.02.011>.
- Hawley, J.G., Dymond, J.R., 1988. How much do trees reduce landsliding? *J. Soil Water Conserv.* 43, 495–498.
- He, L.P., Yu, J.Y., Hu, Q.J., Qu, M.F., He, T.J., 2020. Study on crack propagation and shear behavior of weak muddy intercalations submitted to wetting-drying cycles. *Bull. Eng. Geol. Environ.* 79, 4873–4889. <https://doi.org/10.1007/s10064-020-01842-7>.
- Heckmann, T., Gegg, K., Gegg, A., Becht, M., 2014. Sample size matters: investigating the effect of sample size on a logistic regression susceptibility model for debris flows. *Nat. Hazards Earth Syst. Sci.* 14, 259–278. <https://doi.org/10.5194/nhess-14-259-2014>.
- Hicks, D.L., 1989a. Farm conservation measures' effect on hill country erosion: an assessment in the wake of Cyclone Bola. *DSIR Land and Soil Sciences Technical Record PN 3*. DSIR, Palmerston North.
- Hicks, D.L., 1989b. Storm damage to bush, pasture and forest: some evidence from Cyclone Bola. *DSIR Land Resources Technical Record PN2*. DSIR, Palmerston North.
- Hicks, D.L., 1992. Impact of soil conservation on storm-damaged hill grazing lands in New Zealand. *Aust. J. Soil Water Conserv.* 5, 34–40.
- Hijmans, R.J., 2020. Raster: geographic data analysis and modeling. <https://CRAN.R-project.org/package=raster> R package version 3.4-5.
- Holcombe, E., Smith, S., Wright, E., Anderson, M.G., 2012. An integrated approach for evaluating the effectiveness of landslide risk reduction in unplanned communities in the Caribbean. *Nat. Hazards* <https://doi.org/10.1007/s11069-011-9920-7>.
- Hong, H., Ilia, I., Tsangaratos, P., Chen, W., Xu, C., 2017. A hybrid fuzzy weight of evidence method in landslide susceptibility analysis on the Wuyuan area, China. *Geomorphology* 290, 1–16. <https://doi.org/10.1016/j.geomorph.2017.04.002>.
- Hosmer, D.W., Lemeshow, S., 2000. *Applied Logistic Regression*. Wiley, New York, NY.
- Huang, Y., Zhao, L., 2018. Review on landslide susceptibility mapping using support vector machines. *Catena* 165, 520–529. <https://doi.org/10.1016/j.catena.2018.03.003>.
- Istanbuluoglu, E., Bras, R.L., 2005. Vegetation-modulated landscape evolution: effects of vegetation on landscape processes, drainage density, and topography. *J. Geophys. Res. Earth Surf.* 110, 1–19. <https://doi.org/10.1029/2004JF000249>.
- Kim, D., Im, S., Lee, C., Woo, C., 2013. Modeling the contribution of trees to shallow landslide development in a steep, forested watershed. *Ecol. Eng.* 61, 658–668. <https://doi.org/10.1016/j.ecoleng.2013.05.003>.

- Knevels, R., Petschko, H., Proske, H., Leopold, P., Maraun, D., Brenning, A., 2020. Event-based landslide modeling in the Styrian Basin, Austria: accounting for time-varying rainfall and land cover, pp. 1–29. <https://doi.org/10.3390/geosciences10060217>.
- Kuhn, M., 2008. *Caret package*. *J. Stat. Softw.* 28 (5).
- Lambert, M.G., Trustrum, N.A., Costall, D.A., 1984. Effect of soil slip erosion on seasonally dry Wairarapa hill pastures. *N. Z. J. Agric. Res.* 27, 57–64. <https://doi.org/10.1080/00288233.1984.10425732>.
- Lee, J.M., Begg, J.G., 2002. *Geology of the Wairarapa area*. Institute of Geological & Nuclear Sciences 1:250000 geological map II. 1 sheet + 66 p. Institute of Geological & Nuclear Sciences Limited, Lower Hutt, New Zealand.
- Liu, J.K., Shih, P.T.Y., 2013. Topographic correction of wind-driven rainfall for landslide analysis in Central Taiwan with validation from aerial and satellite optical images. *Remote Sens.* 5, 2571–2589. <https://doi.org/10.3390/rs5062571>.
- Lombardo, L., Mai, P.M., 2018. Presenting logistic regression-based landslide susceptibility results. *Eng. Geol.* 244, 14–24. <https://doi.org/10.1016/j.enggeo.2018.07.019>.
- Marden, M., Herzig, A., Basher, L., 2014. Erosion process contribution to sediment yield before and after the establishment of exotic forest: Waipaoa catchment, New Zealand. *Geomorphology* 226, 162–174. <https://doi.org/10.1016/j.geomorph.2014.08.007>.
- Masi, E.B., Segoni, S., Tofani, V., 2021. Root reinforcement in slope stability models: a review. *Geosciences* 11, 212. <https://doi.org/10.3390/geosciences11050212>.
- McDowell, R.W., Monaghan, R.M., Smith, C., Manderson, A., Basher, L., Burger, D.F., Laurenson, S., Pletnyakov, P., Spiekermann, R., Depree, C., 2020. Quantifying contaminant losses to water from pastoral land uses in New Zealand III. What could be achieved by 2035? *N. Z. J. Agric. Res.* 1–21. <https://doi.org/10.1080/00288233.2020.1844763>.
- McIvor, I., Douglas, G., Dymond, J., Eyles, G., Marde, M., 2011. Pastoral hill slope erosion in New Zealand and the role of poplar and willow trees in its reduction. *Soil Eros. Issues Agric.* <https://doi.org/10.5772/24365>.
- McIvor, I., Clarke, K., Douglas, G., 2015. Effectiveness of conservation trees in reducing erosion following a storm event. In: Currie, L.D., Burkitt, L.L. (Eds.), *Proceedings, 28th Annual Fertiliser and Lime Research Centre Workshop 'Moving farm systems to improved attenuation'*, 8–9 February 2007. Occasional Report 28. Fertiliser and Lime Research Centre, Palmerston North.
- Monaghan, R., Manderson, A., Basher, L., Spiekermann, R., Dymond, J., Smith, C., Muirhead, R., Burger, D., McDowell, R., 2021. Quantifying contaminant losses to water from pastoral landuses in New Zealand II. The effects of some farm mitigation actions over the past two decades. *N. Z. J. Agric. Res.* 1–25. <https://doi.org/10.1080/00288233.2021.1876741>.
- Muenchow, J., Schratz, P., Brenning, A., 2017. RQGIS: Integrating R with QGIS. Retrieved from *R J.* 9 (2), 409–428. <https://cran.r-project.org/package=RQGIS>.
- Neverman, A., Djanibekov, U., Soliman, T., Walsh, P., Spiekermann, R., Basher, L., 2019. Impact testing of a proposed sediment attribute: Identifying erosion and sediment control mitigations to meet proposed sediment attribute bottom lines and the costs and benefits of those mitigations Client report prepared by Manaaki Whenua – Landcare Research for Ministry for the Environment, Report LC3574. <https://www.mfe.govt.nz/sites/default/files/media/Fresh%20water/impact-testing-of-proposed-sediment-attribute.pdf>.
- Newsome, P., Wilde, R., Willoughby, E., 2008. *Land Resource Information System Spatial Data Layers Data Dictionary*. Landcare Research NZ Ltd, Palmerston North, NZ.
- O'Brien, R.M., 2007. A caution regarding rules of thumb for variance inflation factors. *Qual. Quant.* 41, 673–690. <https://doi.org/10.1007/s1135-006-9018-6>.
- Papathoma-Köhle, M., Glade, T., 2013. *The role of vegetation cover change for landslide hazard and risk. The Role of Ecosystems in Disaster Risk Reduction*. UNU-Press, Tokyo, Japan, pp. 293–320.
- Persichillo, M.G., Bordoni, M., Meisina, C., 2017. The role of land use changes in the distribution of shallow landslides. *Sci. Total Environ.* 574, 924–937. <https://doi.org/10.1016/j.scitotenv.2016.09.125>.
- Petschko, H., Brenning, A., Bell, R., Goetz, J., Glade, T., 2014. Assessing the quality of landslide susceptibility maps – case study Lower Austria. *Nat. Hazards Earth Syst. Sci.* 14 (1), 95–118. <https://doi.org/10.5194/nhess-14-95-2014>.
- Phillips, C.J., Marden, M., 2005. *Reforestation schemes to manage regional landslide risk. Landslide Hazard and Risk*. John Wiley & Sons Ltd, Hoboken, NJ.
- Phillips, C., Marden, M., Douglas, G., McIvor, I., Ekanayake, J., 2008. *Decision support for sustainable land management: effectiveness of wide-spaced trees*. Landcare Research Contract Report LC0708/126 for Ministry of Agriculture and Forestry.
- Phillips, C.J., Ekanayake, J.C., Marden, M., 2011. Root site occupancy modelling of young New Zealand native plants: Implications for soil reinforcement. *Plant Soil* 346, 201–214. <https://doi.org/10.1007/s1104-011-0810-2>.
- Phillips, C.J., Marden, M., Suzanne, L.M., 2014. Observations of root growth of young poplar and willow planting types. *N. Z. J. Forest. Sci.* 44 (1), 1–12. <https://doi.org/10.1186/s40490-014-0015-6>.
- Phillips, C., Marden, M., Basher, L.R., 2018. Geomorphology and forest management in New Zealand's erodible steepplands: an overview. *Geomorphology* 307, 107–121. <https://doi.org/10.1016/j.geomorph.2017.07.031>.
- Pisano, L., Zumpano, V., Malek, Rosskopf, C.M., Parise, M., 2017. Variations in the susceptibility to landslides, as a consequence of land cover changes: A look to the past, and another towards the future. *Sci. Total Environ.* 601–602, 1147–1159. <https://doi.org/10.1016/j.scitotenv.2017.05.231>.
- R Core Team, 2021. *R Foundation for Statistical Computing*, Vienna, Austria. <https://www.R-project.org/>.
- Reichenbach, P., Busca, C., Mondini, A.C., Rossi, M., 2014. The influence of land use change on landslide susceptibility zonation: the Briga Catchment Test Site (Messina, Italy). *Environ. Manag.* 54, 1372–1384. <https://doi.org/10.1007/s00267-014-0357-0>.
- Reichenbach, P., Rossi, M., Malamud, B.D., Mihir, M., Guzzetti, F., 2018. A review of statistically-based landslide susceptibility models. *EarthSci. Rev.* 180, 60–91. <https://doi.org/10.1016/j.earscirev.2018.03.001>.
- Rossi, M., Guzzetti, F., Reichenbach, P., Mondini, A.C., Peruccacci, S., 2010. Optimal landslide susceptibility zonation based on multiple forecasts. *Geomorphology* 114, 129–142. <https://doi.org/10.1016/j.geomorph.2009.06.020>.
- Ruff, M., Czurda, K., 2008. Landslide susceptibility analysis with a heuristic approach in the Eastern Alps (Vorarlberg, Austria). *Geomorphology* 94, 314–324. <https://doi.org/10.1016/j.geomorph.2006.10.032>.
- Salter, R.T., Crippen, T.F., Noble, K.E., 1983. *Storm damage assessment of the Thames-Te Aroha area following the storm of April 1981*. Soil Conservation Centre Publication 1. Ministry of Works and Development, Palmerston North, New Zealand.
- Salvatici, T., Tofani, V., Rossi, G., D'Ambrosio, M., Tacconi Stefanelli, C., Benedetta Masi, E., Rosi, A., Pazzi, V., Vannocci, P., Petrolo, M., Catani, F., Ratto, S., Stevenin, H., Casagli, N., 2018. Application of a physically based model to forecast shallow landslides at a regional scale. *Nat. Hazards Earth Syst. Sci.* 18, 1919–1935. <https://doi.org/10.5194/nhess-18-1919-2018>.
- Schmaltz, E.M., Steger, S., Glade, T., 2017. The influence of forest cover on landslide occurrence explored with spatio-temporal information. *Geomorphology* 290, 250–264. <https://doi.org/10.1016/j.geomorph.2017.04.024>.
- Schmidt, K.M., Roering, J.J., Stock, J.D., Dietrich, W.E., Montgomery, D.R., Schaub, T., 2001. The variability of root cohesion as an influence on shallow landslide susceptibility in the Oregon Coast Range. *Can. Geotech. J.* 38, 995–1024. <https://doi.org/10.1139/cgj-38-5-995>.
- Schwarz, M., Preti, F., Giadrossich, F., Lehmann, P., Or, D., 2010. Quantifying the role of vegetation in slope stability: a case study in Tuscany (Italy). *Ecol. Eng.* 36, 285–291. <https://doi.org/10.1016/j.ecoleng.2009.06.014>.
- Schwarz, M., Cohen, D., Or, D., 2012. Spatial characterization of root reinforcement at stand scale: theory and case study. *Geomorphology* 171–172, 190–200. <https://doi.org/10.1016/j.geomorph.2012.05.020>.
- Schwarz, M., Phillips, C., Marden, M., McIvor, I.R., Douglas, G.B., Watson, A., 2016. Modelling of root reinforcement and erosion control by 'Veronese' poplar on pastoral hill country in New Zealand. *N. Z. J. For. Sci.* 46, 1–17. <https://doi.org/10.1186/s40490-016-0060-4>.
- Smith, H.G., Spiekermann, R., Betts, H., Neverman, A.J., 2021. Comparing methods of landslide data acquisition and susceptibility modelling: examples from New Zealand. *Geomorphology* 107660.
- Song, R.H., Hiromu, D., Kazutoki, A., Usio, K., Sumio, M., 2008. Modeling the potential distribution of shallow-seated landslides using the weights of evidence method and a logistic regression model: a case study of the Sabae Area, Japan. 23, 106–118. [https://doi.org/10.1016/S1001-6279\(08\)60010-4](https://doi.org/10.1016/S1001-6279(08)60010-4).
- Spiekermann, R.I., McColl, S., Fuller, I., Dymond, J., Burkitt, L., Smith, H.G., 2021. Quantifying the influence of individual trees on slope stability at landscape scale. *J. Environ. Manag.* 286, 112194. <https://doi.org/10.1016/j.jenvman.2021.112194>.
- Steger, S., Brenning, A., Bell, R., Petschko, H., Glade, T., 2016a. Exploring discrepancies between quantitative validation results and the geomorphic plausibility of statistical landslide susceptibility maps. *Geomorphology* 262, 8–23. <https://doi.org/10.1016/j.geomorph.2016.03.015>.
- Steger, S., Brenning, A., Bell, R., Glade, T., 2016b. The propagation of inventory-based positional errors into statistical landslide susceptibility models. *Nat. Hazards Earth Syst. Sci.* 16, 2729–2745. <https://doi.org/10.5194/nhess-16-2729-2016>.
- Steger, S., Brenning, A., Bell, R., Glade, T., 2017. The influence of systematically incomplete shallow landslide inventories on statistical susceptibility models and suggestions for improvements. *Landslides* 14, 1767–1781. <https://doi.org/10.1007/s10346-017-0820-0>.
- Thompson, R.C., Luckman, P.G., 1993. Performance of biological erosion control in New Zealand soft rock hill terrain. *Agrofor. Syst.* 21, 191–211. <https://doi.org/10.1007/BF00705230>.
- Torizín, J., Wang, L., Fuchs, M., Tong, B., Balzer, D., Wan, L., Kuhn, D., Li, A., Chen, L., 2018. Statistical landslide susceptibility assessment in a dynamic environment: a case study for Lanzhou City, Gansu Province, NW China. *J. Mt. Sci.* 15, 1299–1318. <https://doi.org/10.1007/s11629-017-4717-0>.
- Van Den Eeckhaut, M., Vanwalleghem, T., Poesen, J., Govers, G., Verstraeten, G., Vandekerckhove, L., 2006. Prediction of landslide susceptibility using rare events logistic regression: a case-study in the Flemish Ardennes (Belgium). *Geomorphology* 76, 392–410. <https://doi.org/10.1016/j.geomorph.2005.12.003>.
- van Westen, C.J., Castellanos, E., Kuriakose, S.L., 2008. Spatial data for landslide susceptibility, hazard, and vulnerability assessment: an overview. *Eng. Geol.* 102, 112–131. <https://doi.org/10.1016/j.enggeo.2008.03.010>.
- van Zadelhoff, F.B., Albaba, A., Cohen, D., Phillips, C., Schaeffli, B., Dorren, L.K.A., Schwarz, M., 2021. Introducing SlideforMap: a probabilistic finite slope approach for modelling shallow landslide probability in forested situations. *Nat. Hazards Earth Syst. Sci. Discuss.* 2021, 1–33. <https://doi.org/10.5194/nhess-2021-140>.
- Wairarapa Catchment Board, 1956. *Farm conservation scheme 16/F.P./32*. Greater Wellington Regional Council.
- Walker, S.H., Duncan, D.B., 1967. Estimation of the probability of an event as a function of several independent variables. *Biometrika* 54, 167–178.
- Watson, A.J., Marden, M., 2004. Live root-wood tensile strengths of some common New Zealand indigenous and plantation tree species. *N. Z. J. For. Sci.* 34, 344–353.
- Watson, A., Marden, M., Rowan, D., 1995. Tree species performance and slope stability. *veg. slopes stabilisation*. *Prot. Ecol.*, 161–171. <https://doi.org/10.1680/vasspae.20313.0018>.
- Weinstein B.G., Ben, Marconi, Sergio, Bohlman S.A., Stephanie, Zare, Alina, Singh, Aditya, Graves S.J., Sarah, White E.P., Ethan, 2021. A remote sensing derived data set of 100 million individual tree crowns for the national ecological observatory network. *eLife* 10, 1–18. <https://doi.org/10.7554/eLife.62922>.

- Weisberg, S., Fox, J., 2010. *An R companion to applied regression*. Sage Publications, Los Angeles, London, New Delhi, Singapore, Washington, D.C.
- Wilkinson, A., 1999. Poplars and willows for soil erosion control in New Zealand. *Biomass Bioenergy* 16, 263–274. [https://doi.org/10.1016/S0961-9534\(99\)00007-0](https://doi.org/10.1016/S0961-9534(99)00007-0).
- Wu, W., Sidle, R.C., 1995. A distributed slope stability model for steep forested basins. *Water Resources Research* 31, 2097–2110.
- Xiao, T., Segoni, S., Chen, L., Yin, K., Casagli, N., 2020. A step beyond landslide susceptibility maps: a simple method to investigate and explain the different outcomes obtained by different approaches. *Landslides* 17, 627–640. <https://doi.org/10.1007/s10346-019-01299-0>.